Chem Soc Rev

REVIEW ARTICLE

View Article Online
View Journal

Check for updates

Cite this: DOI: 10.1039/d5cs01218j

Catalytic asymmetric [4+2] cycloadditions of unsaturated hydrocarbons by transition metal catalysis and photocatalysis

Jun-Xiong He and Quan Cai *

The enantioselective Diels–Alder reaction is arguably one of the most efficient and straightforward approaches for the construction of chiral six-membered carbocycles. However, the generality of this conventional reaction is limited by restrictive electronic requirements and substitution patterns according to the classic Hoffmann–Woodward rules. To circumvent these limitations, several innovative approaches have emerged in recent years. Using these approaches, various types of electronic mismatched [4+2] cycloadditions of unsaturated carbons, such as alkenes, alkynes, and allenes, have been realized. This review will summarize these advancements in this rapidly growing area within the past three decades, including the transition metal-catalyzed asymmetric [4+2] cycloadditions *via* the oxidative cyclometallation and reductive elimination pathway, catalytic asymmetric [4+2] cycloadditions *via* the LUMO activation by π-acids and the HOMO activation by π-bases, as well as catalytic asymmetric radical-mediated [4+2] cycloadditions under light irradiation.

Received 14th October 2025

DOI: 10.1039/d5cs01218j

rsc.li/chem-soc-rev

Open Access Article. Published on 13 2026. Downloaded on 08/05/26 22:54:22.
This article is licensed under a Creative Commons Attribution 3.0 Unported Licence.

1. Introduction

Six-membered ring structures are widely distributed in natural products, pharmaceuticals, and organic materials.[1–4] Consequently, the development of methodologies for the synthesis of six-membered rings is a central theme in organic synthesis. From the synthetic perspective, the Diels–Alder reaction, which was first discovered by Otto Diels and Kurt Alder in 1928,[5] is unambiguously one of the most efficient methods for the construction of six-membered rings.[6–13] Using readily available 1,3-dienes and alkene/alkyne dienophiles as reaction components, this reaction could construct a new six-membered ring by forming two new bonds with

Department of Chemistry, Research Center for Molecular Recognition and Synthesis, State Key Laboratory of Green Chemical Synthesis and Conversion, Fudan University, Shanghai 200433, China. E-mail: quan_cai@fudan.edu.cn

Jun-Xiong He

Jun-Xiong He received his BSc degree from Jiangxi Normal University in 2018 and MSc from East China Normal University in 2021 under the supervision of Prof. Jian Zhou. Then, he earned his PhD degree in chemistry from Fudan University in 2025 under the supervision of Prof. Quan Cai. He is now working as a postdoctoral fellow in the lab of Prof. Shu-Li You at the Shanghai Institute of Organic Chemistry.

Quan Cai

Quan Cai received his BSc degree from the East China University of Science and Technology (2007) and his PhD degree from the Shanghai Institute of Organic Chemistry with Prof. Shu-Li You (2012). After postdoctoral work with Prof. K. C. Nicolaou at the Scripps Research Institute and Rice University (2012–2016) and with Prof. Nathanael Gray at Dana-Farber Cancer Institute, Harvard Medical School (2016–2017), he joined the Department of Chemistry at Fudan University as a tenure-track professor. In 2022, he was promoted to a full professor. His current research focuses on asymmetric catalysis, transition-metal catalysis, and total synthesis of natural products.

Open Access Article. Published on 13 2026. Downloaded on 08/05/26 22:54:22.
This article is licensed under a Creative Commons Attribution 3.0 Unported Licence.

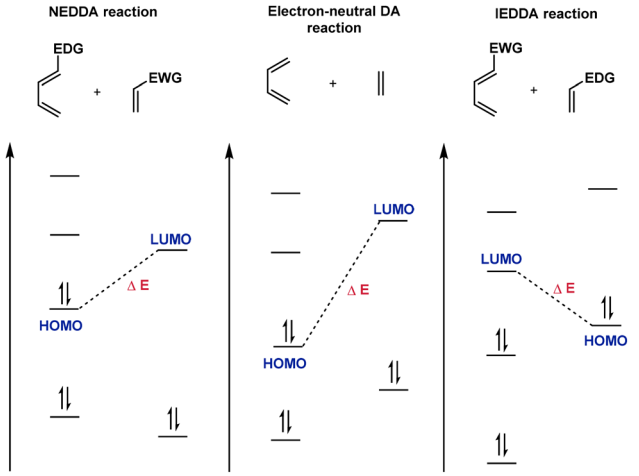

Scheme 1 Classification of Diels–Alder reactions. NEDDA reactions, normal-electron-demand Diels–Alder reactions; IEDDA reactions, inverse-electron-demand Diels–Alder reactions; HOMO, highest occupied molecular orbital; LUMO, lowest unoccupied molecular orbital; EDG, electron-donating group; and EWG, electron-withdrawing group.

up to four stereogenic centers in a single step. The popularity of this reaction in synthesis is not only credited to its ability to construct complex ring systems but also to the predictable regioselectivity and diastereoselectivity, thereby highly reinforcing its reliability in targeted synthesis.

In general, Diels–Alder reactions are classified into three types: NEDDA reactions, IEDDA reactions, and electron-neutral Diels–Alder reactions (Scheme 1).[14–16] According to the classic FMO (frontier molecular orbital) theory,[17–19] NEDDA reactions are dominated by the energy gap between the HOMO of electron-rich dienes and the LUMO of electron-deficient dienophiles, while IEDDA reactions are controlled by the LUMO/HOMO interaction between electron-deficient dienes and electron-rich dienophiles. Compared with electron-neutral reactions, both NEDDA reactions and IEDDA reactions are facile to occur owing to the narrowed energy gap. Based on these modes, an appropriate chiral catalyst could be utilized to increase the HOMO energy or decrease the LUMO energy of reaction components, thus enhancing the reaction rate and controlling the stereoselectivity.

Since the first aluminum-catalyzed asymmetric Diels–Alder reaction discovered by Koga in 1979 (Scheme 2A),[20,21] the synthetic community has witnessed great progress in the development of efficient catalytic systems to facilitate enantioselective Diels–Alder reactions, including the use of Lewis acids, biocatalysts, chiral Brønsted acids, chiral amines, and other organocatalytic systems.[22–37] Despite significant advancements that have been achieved, the applicability of asymmetric Diels–Alder reactions in organic synthesis is severely limited by the requirement of restrictive electronic complementarity between dienes and dienophiles. In addition, the reaction partners need to be equipped with polar functional groups to provide binding sites for catalysts, thus further narrowing the application scope (Scheme 2B).

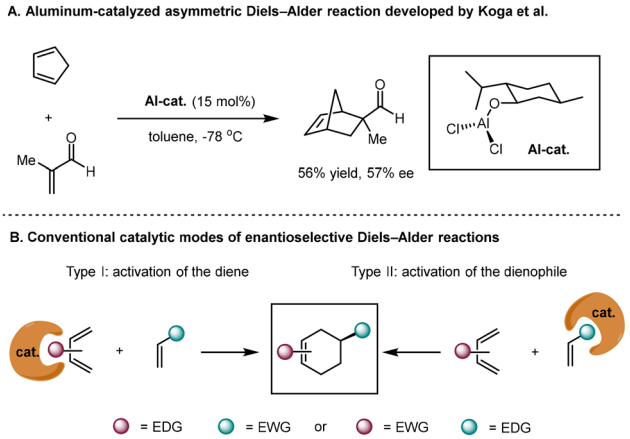

Scheme 2 Conventional catalytic asymmetric Diels–Alder reactions.

To circumvent these limitations, several innovative approaches have been developed. Notably, transition metal-catalyzed cycloadditions of alkenes, alkynes, or allenes *via* the oxidative cyclometallation followed by the reductive elimination reaction pathway could overcome certain limitations of pericyclic cycloadditions.[38–43] This reaction mode enables unactivated unsaturated hydrocarbons to participate in [4+2] cycloadditions that otherwise need to occur under harsh reaction conditions (Scheme 3A). On the other hand, by the coordination with a π-acid such as the gold(I) complex, the LUMO energy of C–C double or triple bonds can be lowered,[44–50] thus facilitating efficient [4+2] cycloadditions with complementary reaction partners (Scheme 3B). More recently, a novel π-Lewis base

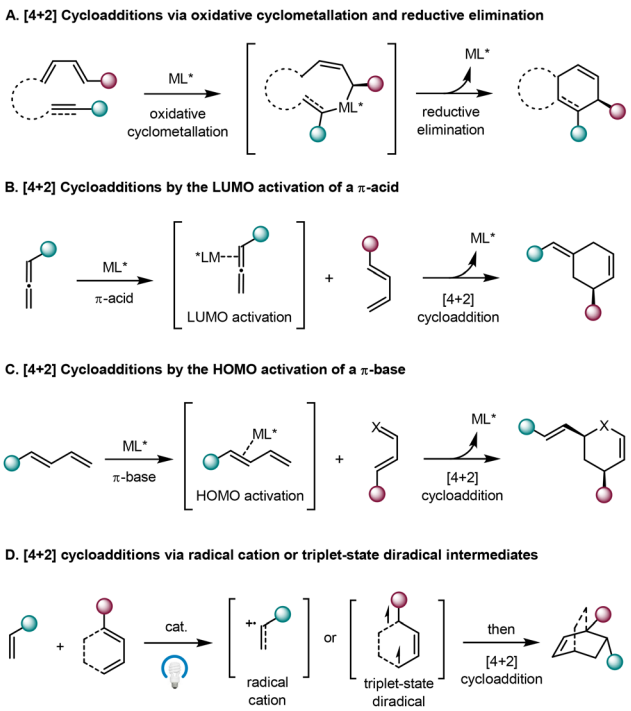

Scheme 3 New approaches for catalytic asymmetric [4+2] cycloadditions of alkenes, alkynes and allenes.

This journal is © The Royal Society of Chemistry 2026

Open Access Article. Published on 13 2026. Downloaded on 08/05/26 22:54:22.
This article is licensed under a Creative Commons Attribution 3.0 Unported Licence.

catalytic strategy has been devised.[51] It has been demonstrated that low-valent transition metal complexes could serve as π-Lewis bases to raise the HOMO energy of 1,3-dienes by π-backdonation upon η^2 coordination, thereby promoting [4+2] cycloadditions with electron-deficient diene components (Scheme 3C). Particularly noteworthy are photocycloaddition reactions, which have gained significant attention owing to their ability to mediate reactions between simple olefins under mild conditions.[52–57] In this rapidly growing field, catalytic asymmetric photoinduced [4+2] cycloadditions through radical reaction pathways have also emerged (Scheme 3D).

In recent years, numerous excellent review articles on [4+2] cycloadditions have been reported. However, most of them have been predominantly devoted to conventional catalytic asymmetric Diels–Alder reactions.[22–35] Given the fact that great progress in transition metal catalysis and photocatalysis has been realized in the past three decades, it is a good occasion to summarize the exciting advancements in the development of catalytic asymmetric [4+2] cycloadditions of unsaturated hydrocarbons (alkenes, alkynes and allenes) through these novel approaches. The aim of this review is to provide a concise overview of this research field to readers. According to the above discussion (Scheme 3), this review is organized into four sections based on catalytic activation modes: (1) catalytic asymmetric [4+2] cycloadditions *via* the oxidative cyclometallation and reductive elimination pathways, (2) enantioselective [4+2] cycloadditions *via* the LUMO activation of π-acids, (3) enantioselective [4+2] cycloadditions *via* the HOMO activation of π-bases, and (4) catalytic asymmetric radical-mediated [4+2] cycloadditions.

2. Catalytic asymmetric [4+2] cycloadditions *via* the oxidative cyclometallation/reductive elimination pathway

The Diels–Alder reaction plays a pivotal role in the construction of six-membered rings, rendering it one of the most extensively employed methodologies in organic synthesis. According to FMO rules, this reaction is facile to occur within electronically complementary components. Actually, the inherent reluctance of electronically similar reactants to undergo cyclization under ambient conditions still represents one of the most significant limitations for this remarkable reaction. In this regard, transition metal catalysts can accelerate [4+2] cycloadditions between electronically similar reaction components *via* oxidative cyclometallation and subsequent reductive elimination. Notably, great progress in catalytic asymmetric [4+2] cycloadditions of electronically unbiased hydrocarbons has been achieved by a diverse range of transition metals such as Rh, Pd, Ru, Ni, Fe, and Co. In this section, we will discuss the advancements in this area according to transition metals.

2.1. Rh-catalyzed [4+2] cycloadditions

In 1990, Livinghouse *et al.* reported the Rh(I)-catalyzed intramolecular [4+2] cycloadditions of unactivated diene-ynes **1**

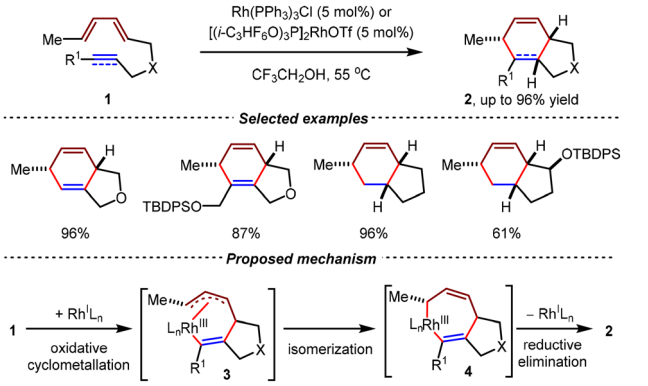

Scheme 4 Rhodium(I)-catalyzed intramolecular [4+2] cycloadditions of diene-ynes and trienes.

(Scheme 4).[58] By the catalysis of commercially available Rh(I) complexes $[(PPh_3)_3RhCl]$ or $[(i\text{-}C_3HF_6O)_3P]_2RhOTf$, several types of 5/6 bicyclic ring scaffolds **2** were efficiently constructed with high yields under mild conditions. Moreover, terminal triene substrates also demonstrated excellent compatibility, affording the corresponding bicyclic adducts with moderate to high yields. In this study, a reasonable mechanism was suggested. The catalytic cycle was initiated by the coordination of substrate **1** and the Rh(I) complex, which then formed the allylic η^3-coordinated Rh(III) complex **3** by oxidative cyclometallation. Subsequently, this intermediate underwent allylic isomerization to yield Rh(III) species **4**, which ultimately proceeded reductive elimination to furnish the final product **2**.

Based on this study, the same group realized the first Rh(I)-catalyzed intramolecular asymmetric [4+2] cycloadditions in 1994.[59] Using DIOP-type bisphosphines **L1** as chiral ligands, 5/6 bicyclic products with diverse substitution patterns were obtained enantioselectively from unactivated triene and diene-yne substrates **5** in good yields with up to 87% ee (Scheme 5). Although only moderate enantioselectivities were observed in some examples, this seminal work laid the foundation for the subsequent exploration of transition metal-mediated stereoselective annulations.

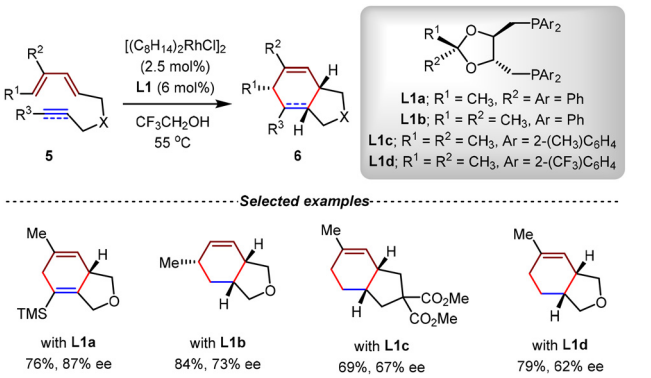

Scheme 5 Rhodium(I)-catalyzed asymmetric intramolecular [4+2] cycloadditions of diene-ynes and trienes.

Open Access Article. Published on 13 2026. Downloaded on 08/05/26 22:54:22.
This article is licensed under a Creative Commons Attribution 3.0 Unported Licence.

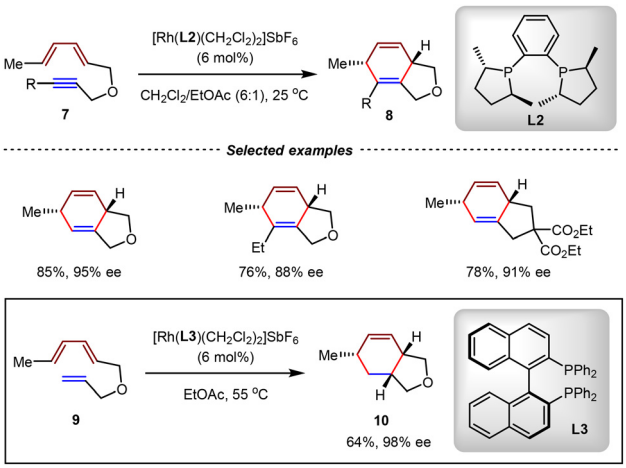

Scheme 6 Asymmetric intramolecular [4+2] cycloadditions catalyzed by a rhodium(I)/DUPHOS complex or rhodium(I)/BINAP complex.

It has been found that the counterion of the rhodium catalyst had a significant influence on the reactivity and stereocontrol in [4+2] cycloadditions. Using Rh(I) catalysts bearing hexafluoroantimonate (SbF_6^-) as the counterion, the Gilbertson group investigated the performance of various chiral biphosphine ligands in [4+2] cycloadditions.[60,61] The utilization of DUPHOS **L2** as the ligand was found to be effective in intramolecular asymmetric [4+2] cycloadditions of diene-yne substrates **7**, affording products **8** in high yields (76–85%) and high enantioselectivities (88–95% ee) (Scheme 6). Remarkably, the utilization of BINAP **L3** enabled the [4+2] cycloaddition of triene **9** with comparable efficiency, delivering cycloadduct **10** in 64% yield and 98% ee. This study demonstrated the critical role of chiral phosphines in achieving good reactivity and enantiocontrol in transition metal-catalyzed [4+2] cycloadditions.

In 2001, Livinghouse and coworkers synthesized a series of *P*-chirogenic diphosphine ligands and evaluated them in the cationic Rh(I)-catalyzed intramolecular [4+2] cycloaddition of nitrogen-tethered triene **11**.[62] The phosphine linking element showed a great influence on the enantioselectivity. When diisopropylsila-bridged *P*-chirogenic diphosphine ligand **L4** was employed, the desired hexahydroisoindole product **12** was obtained in 85% yield and 91% ee (Scheme 7).

The Schmalz group developed a cationic rhodium-catalyzed enantioselective intramolecular [4+2] cycloaddition using TADDOL-derived phosphine–phosphite **L5** bearing a phenyl group adjacent to the phosphite moiety as the chiral ligand (Scheme 8).[63] By this method, 5/6-bicyclic products **14** were obtained as single diastereoisomers in good to excellent

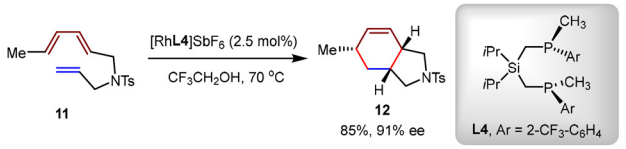

Scheme 7 Rhodium(I)-catalyzed asymmetric intramolecular [4+2] cycloaddition of the nitrogen-tethered triene.

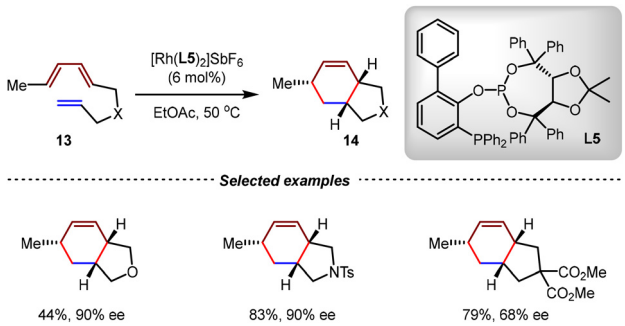

Scheme 8 Asymmetric intramolecular [4+2] cycloadditions of unactivated trienes catalyzed by a rhodium(I)/TADDOL-derived phosphine–phosphite ligand complex.

enantioselectivities (up to 93% ee) from diene-enes **13**. The key to realize high enantioselectivities was the preparation of the "aged" catalyst by microwave irradiation of the pre-catalyst from $[Rh(NBD)Cl]_2$, $AgSbF_6$, and **L5** (0.5 : 1 : 1.6). Mechanistic studies including ^{31}P NMR and ESI-MS measurements suggested that the $[Rh(L5)_2]^+$ species was a more selective catalyst.

In previous studies, the Rh(I) catalysts were typically generated *in situ* from achiral Rh(I)/diene complexes and chiral phosphine ligands. However, the effect of diene ligands in reactions had been ignored for many years. In 2006, the Mikami group disclosed the asymmetric synergistic effect between the chiral diene and diphosphine ligands (Scheme 9).[64] By the combination of $[Rh(L7)Cl]_2$, DUPHOS ligand **L6** and $AgSbF_6$, 5/6-bicyclic products **16** were synthesized with high yields and

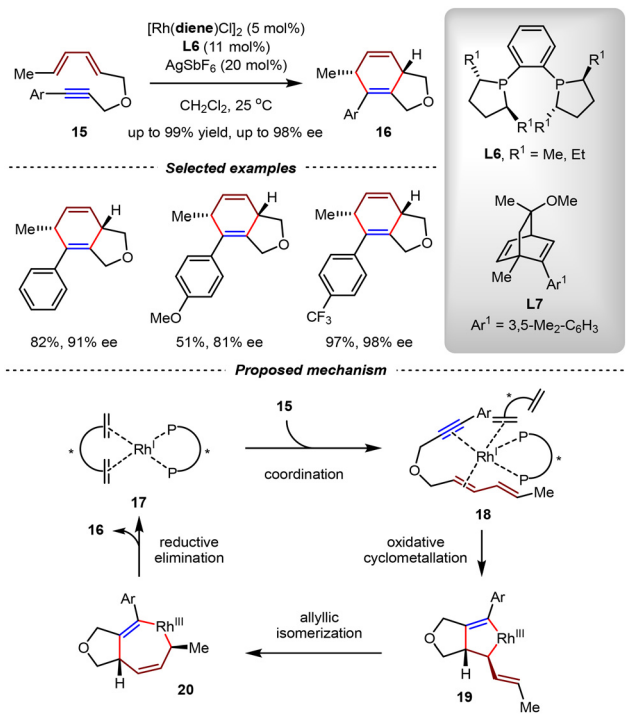

Scheme 9 Asymmetric intramolecular [4+2] cycloadditions catalyzed by a rhodium(I)/DUPHOS/diene complex.

This journal is © The Royal Society of Chemistry 2026

Open Access Article. Published on 13 2026. Downloaded on 08/05/26 22:54:22.
This article is licensed under a Creative Commons Attribution 3.0 Unported Licence.

enantioselectivities (up to 99% yield, 98% ee) from unactivated diene-ynes *via* intramolecular [4+2] cycloadditions. It should be noted that the sole utilization of diphosphine ligand **L6** or diene ligand **L7** led to the desired cycloadducts in low enantioselectivities. In a plausible mechanism, the Rh(I)/**L6**/**L7** complex was proposed as the active catalyst. The catalytic cycle was initiated by the coordination of **17** with diene-yne **15**. The resulting intermediate **18** was further transformed into **19** by oxidative cyclometallation. Subsequently, this intermediate underwent allylic rhodium(III) isomerization to yield intermediate **20**. From **20**, the reductive elimination led to the final product **16** and regenerated the active Rh(I) catalyst **17**. In the structure of the key intermediate **18**, the diene ligand was proposed to coordinate with the metal center *via* η^2 coordination, while the biphosphine ligand complexed with the metal center *via* η^4 coordination.

Chung *et al.* demonstrated that the phosphine-free rhodium(I)/diene complex [Rh(naphthalene)(cod)]BF_4 could act as an effective catalyst to promote intermolecular and intramolecular [4+2] cycloadditions between unactivated 1,3-dienes and alkynes.[65] However, only racemic products were afforded by this achiral catalytic system. In 2007, Shintani and Hayashi *et al.* realized the cationic Rh(I)-catalyzed asymmetric intramolecular [4+2] cycloaddition of diene-yne by the sole utilization of diene (*S*,*S*)-Ph-bicyclo[2.2.2]octadiene (bod*) **L8** (Scheme 10).[66] By this catalytic system, [4+2] cycloadditions of both aryl- and alkyl-terminated diene-ynes **21** proceeded smoothly, affording the desired cycloadducts **22** in high yields (up to 96%) with excellent enantioselectivities (up to 99% ee). Notably, the intermolecular [4+2] cycloaddition between 1,3-dienes **23** and electron-deficient alkyne **24** was also compatible, giving 1,4-cyclohexadienes **25** in good yields and enantioselectivities. By direct comparison, the diene ligand showed much higher reactivity than phosphine ligands in this Rh(I)-catalyzed [4+2] cycloaddition.

In 2008, the Shibata group reported the intermolecular asymmetric [4+2] cycloadditions of 1,3-dienes with dimethyl acetylenedicarbonate (DMAD) **24**. Using [Rh(cod)**L3**]BF_4 as the chiral catalyst, a variety of 1,4-cyclohexadienes were obtained in moderate yields and good enantioselectivities (up to 66% yield, 94% ee) (Scheme 11).[67] Notably, 1,1-disubstituted 1,3-butadiene was compatible, giving the corresponding 1,4-cyclohexadiene in 47% yield and 87% ee. 1,2-Disubstituted 1,3-butadiene was also viable, and the bicyclic product was produced in 65% yield and 78% ee. In a proposed mechanism, the Rh(I)/**L3** catalyst initially coordinated with 1,3-dienes **26** and DMAD. Since the 3,4-position of the 1-substituted-1,3-diene was less sterically hindered than the 1,2-position, the subsequent oxidative cyclometallation occurred at the 3,4-position of **26** with the alkyne moiety of DMAD. Due to the steric repulsion between the methoxycarbonyl and alkenyl groups in intermediate **30**, metallacyclopentene **29** was therefore preferentially formed, which then underwent 1,3-allylic rearrangement and reductive elimination to afford the final product **27**.

In 2012, the Tanaka group reported an intermolecular [2+2+2] trimerization/asymmetric intramolecular [4+2] cycloaddition of 5-alkynals **32** and two aryl ethynyl ethers **33**. Using [$Rh(cod)_2$]BF_4/**L9** as the chiral catalyst, a wide range of annulated 1,4-cyclohexadienes **34** were obtained regioselectively and diastereoselectively with up to 67% yield, >99% ee, and >99 : 1 dr (Scheme 12).[68] A plausible mechanism is depicted in Scheme 12. By the catalysis of Rh/**L9**, two molecules of aryl ethynyl ether **33** underwent the oxidative cyclometallation, generating the rhodacyclopentadiene intermediate **35**. Subsequently, insertion of the formyl group of 5-alkynal **32** into **35**

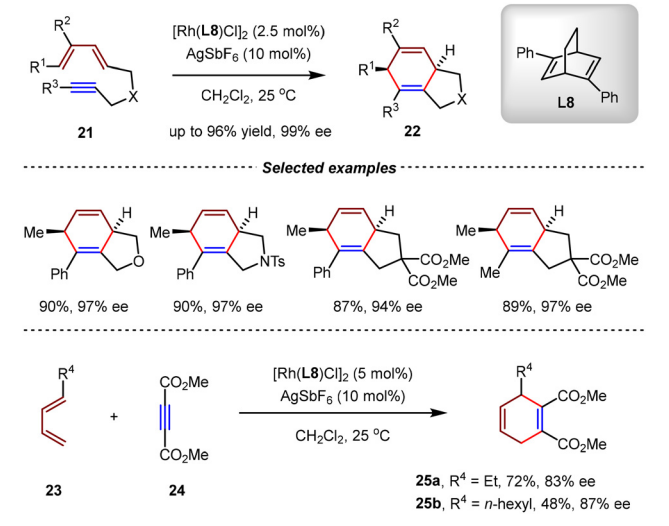

Scheme 10 Rh(I)/chiral diene-catalyzed asymmetric intramolecular and intermolecular [4+2] cycloadditions.

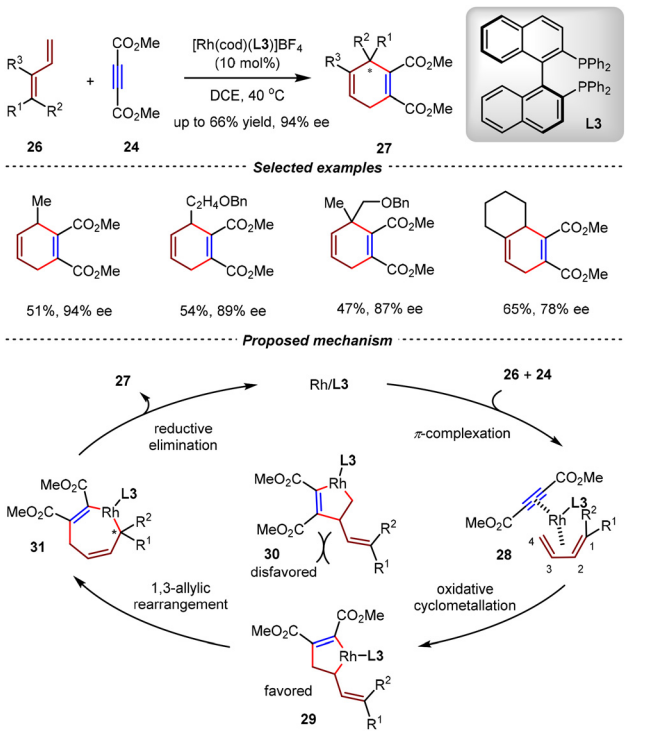

Scheme 11 Rh(I)/BINAP-catalyzed asymmetric intermolecular [4+2] cycloadditions of 1,3-dienes and DMAD.

Open Access Article. Published on 13 2026. Downloaded on 08/05/26 22:54:22.
This article is licensed under a Creative Commons Attribution 3.0 Unported Licence.

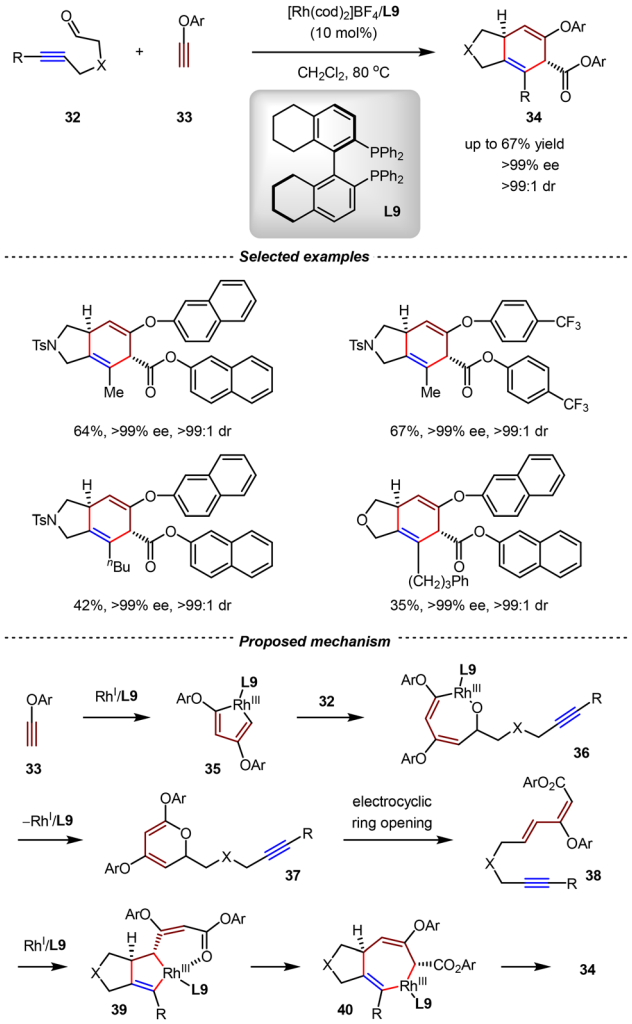

Scheme 12 Rh(I)/(R)-H_8-BINAP-catalyzed intermolecular [2+2+2] trimerization/asymmetric intramolecular [4+2] cycloaddition.

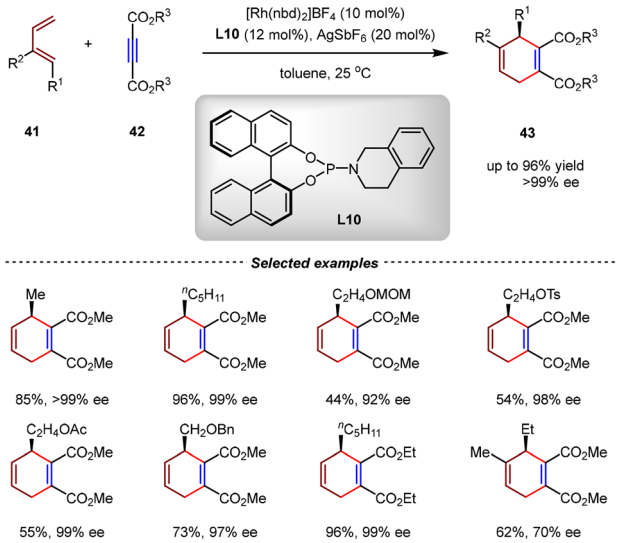

Scheme 13 Rh(I)/phosphomidite-catalyzed asymmetric intermolecular [4+2] cycloadditions of 1,3-dienes and DMADs.

afforded rhodacycle **36**, which then underwent reductive elimination to give pyran derivative **37**. From **37**, the electrocyclic ring-opening delivered dienyne **38**, which then afforded rhodacyclopentene **39** with the rhodium catalyst. The 1,3-allylic migration of **39** followed by the reductive elimination afforded **34** as the final product.

In 2020, Shi *et al.* identified a highly efficient Rh(I) catalytic system to realize the intermolecular [4+2] cycloadditions of 1-substituted-1,3-dienes and DMADs with high enantioselectivities (Scheme 13).[69] Using phosphoramidite **L10** as the chiral ligand, a wide range of cyclohexa-1,4-dienes **43** were obtained with up to 96% yield and >99% ee under mild reaction conditions. A similar mechanism involving the oxidative cyclometallation, 1,3-allylic rearrangement, and reductive elimination was proposed.

The first Rh(I)-catalyzed intramolecular [4+2] cycloadditions of allene-1,3-dienes were reported by the Wender group in 1995.[70,71] By the utilization of phosphites as ligands, [4+2] cycloadditions of 1,3-disubstituted allene-1,3-dienes **44** allowed the construction of 6/5 and 6/6-fused bicyclic ring systems **45** with high yields under mild reaction conditions. Intriguingly, when $P[OCH(CF_3)_2]_2$ was used as the ligand, the cycloaddition of **46** occurred regioselectively on the external double bond of the allene moiety, giving 6/7-fused bicyclic product **47** in 89% yield (Scheme 14).

In 2018, the Ma group realized the $RhCl(PPh_3)_3$-catalyzed intramolecular [4+2] cycloadditions of racemic 1,3-disubstituted allene-1,3-dienes with axial chirality.[72] By the catalysis of $RhCl(PPh_3)_3$ (2.0 mol%), *cis*-fused bicyclic products **49** were produced with up to 87% yields (Scheme 15). The cycloaddition process occurred regioselectively on the internal double bond of the allene moiety. Notably, the configuration of the non-bridging carbon center in the six-membered ring was governed by the configuration of the double bond of the 1,3-diene moiety. When optically active allene-1,3-diene substrate **50**

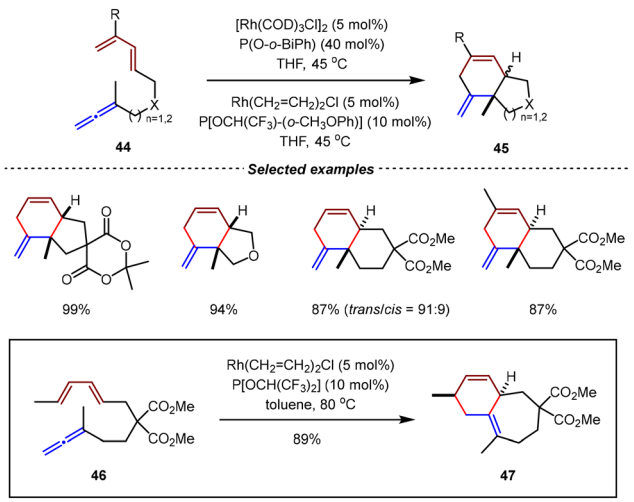

Scheme 14 Rh(I)/phosphite-catalyzed intramolecular [4+2] cycloaddition of 1,1-disubstituted allene-1,3-dienes.

This journal is © The Royal Society of Chemistry 2026

Open Access Article. Published on 13 2026. Downloaded on 08/05/26 22:54:22.
This article is licensed under a Creative Commons Attribution 3.0 Unported Licence.

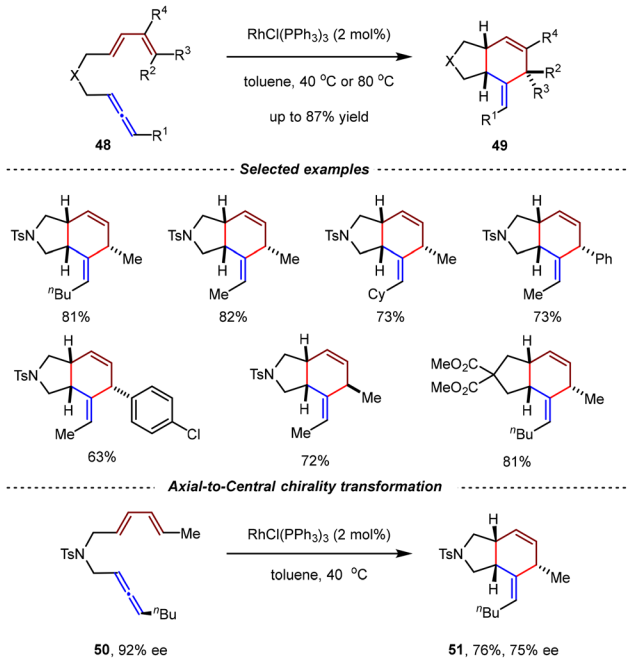

Scheme 15 $RhCl(PPh_3)_3$-catalyzed intramolecular [4+2] cycloadditions of 1,3-disubstituted allene-1,3-dienes.

reacted under standard conditions, the axial-to-central chirality transfer process occurred, giving **51** as a single diastereoisomer in 75% ee.

To improve the efficiency of the axial-to-central chirality transfer process, Ma *et al.* reexamined the Rh(I)-catalyzed intramolecular [4+2] cycloadditions of optically active 1,3-disubstituted allene-1,3-dienes.[73] It was found that when $Rh(PPh_3)_3SbF_6$ was used as the catalyst in ethanol, a complete chirality transfer was observed; the corresponding *cis*-5/6-fused bicyclic adducts **53** were obtained with high yields and retained enantioselectivities (up to 99% ee) (Scheme 16). A series of control experiments indicated that the axial chirality of the 1,3-disubstituted allene moiety governed the absolute configurations of *in situ* generated chiral centers by chirality transfer. In a proposed mechanism, both intermediate **54** and its enantiomeric isomer *ent*-**54** could be formed *via* ligand exchange between allene-1,3-dienes **52** and the *in situ* generated $[Rh(PPh_3)_3]SbF_6$ catalyst. Owing to the significant steric hindrance between the R^1 substituent and the catalyst framework in *ent*-**54**, intermediate **54** was energetically more favored. From **54**, the subsequent cyclometallation and allylic isomerization steps generated rhodabicyclic intermediate **56**, in which the three tertiary hydrogen atoms were positioned in a *cis*-configuration. Finally, reductive elimination followed by ligand exchange with allene-1,3-dienes **52** gave product **53** and regenerated the active catalytic species **54**.

In 2021, the Gilbertson group also investigated the Rh(I)-catalyzed intramolecular [4+2] cycloadditions of chiral allene-1,3-dienes (Scheme 17).[74] It was found that employing $[Rh(cod)Cl]_2$/**L11** as the catalyst in toluene at 80 °C, optically active allene-1,3-dienes **58** (80–98% ee) could be transformed

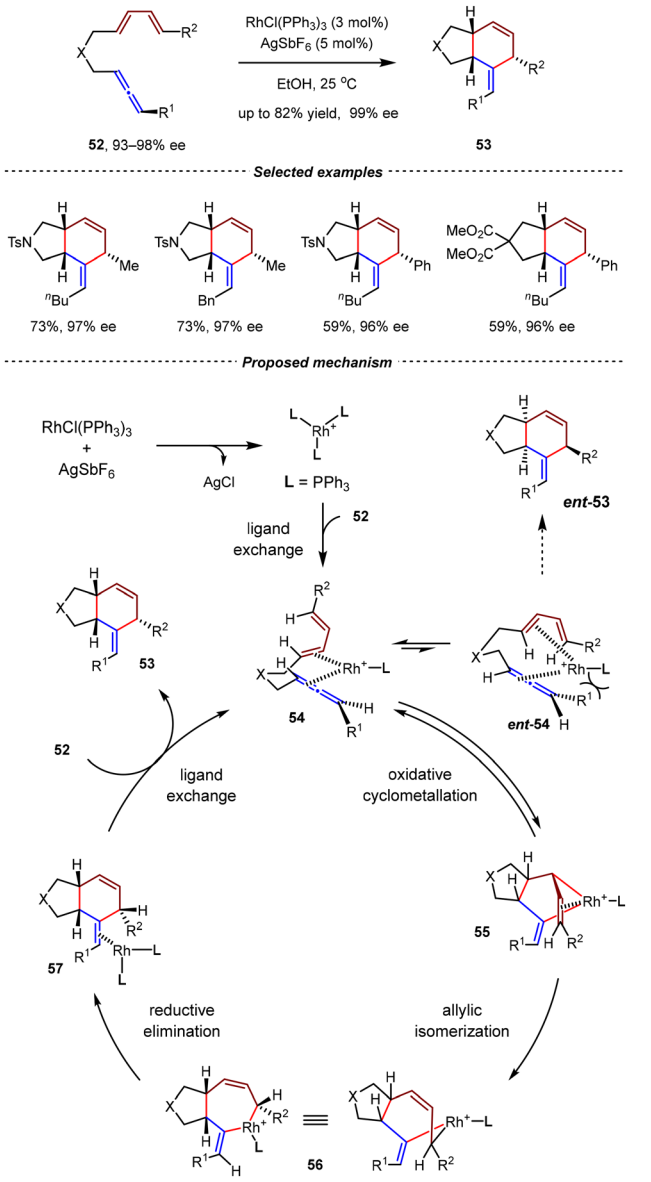

Scheme 16 $Rh(PPh_3)_3SbF_6$-catalyzed intramolecular [4+2] cycloadditions of optical active allene-1,3-dienes.

into **59** with excellent yields and retained enantioselectivities (up to 96% yield, 98% ee). In most cases, the diastereoselectivities ranged from 99 : 1 to 90 : 10. The utilization of phosphine-phosphine oxide ligand **L11** [1,2-bis(diphenylphosphino)ethane oxide, dppeO] was the key for the success of this transformation. It should be noted that optically active allene-1,3-dienes were prepared by the $CuBr_2$-catalyzed EATA (enantioselective allenation of terminal alkynes) reaction developed by Ma and coworkers.[75,76]

In 2021, Ma and coworkers reported the first Rh-catalyzed kinetic resolution-based enantioselective [4+2] cycloaddition-isomerization of 1,3-disubstituted allene-1,3-dienes (Scheme 18).[77] By the catalysis of $[Rh(C_2H_4)_2Cl]_2$ and $AgSbF_6$ with (*R*,*R*)-Ph-BPE **L12** in EtOH at 40 °C, a wide range of aza-[4.3.0]bicyclic compounds **61** bearing various functionalities were synthesized in satisfactory yields (up to 40%) and enantioselectivities (up to >99% ee)

Open Access Article. Published on 13 2026. Downloaded on 08/05/26 22:54:22.
This article is licensed under a Creative Commons Attribution 3.0 Unported Licence.

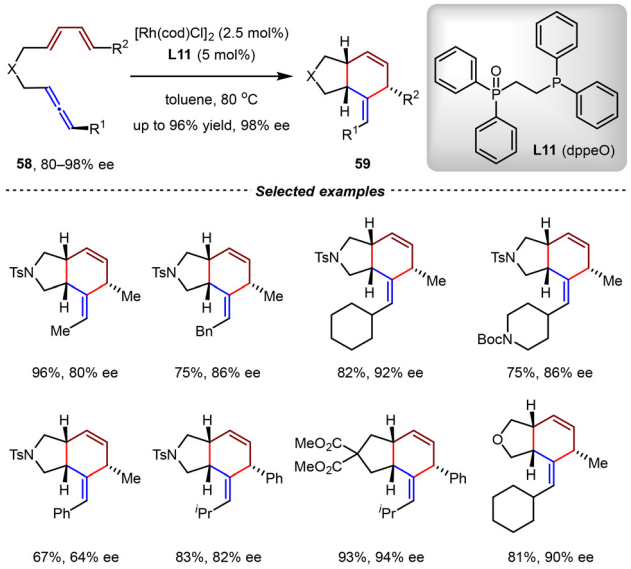

Scheme 17 Rh(I)/dppeO-catalyzed intramolecular [4+2] cycloadditions of optically active allenyl 1,3-dienes.

from racemic 1,3-disubstituted allene-1,3-dienes. Intriguingly, these reactions exhibited a substrate-controlled divergence. While the (*Sa*)-enantiomer of substrate **60** participated in cyclization, the residual (*Ra*)-enantiomer was exclusively transformed into 1,3-diene derivative **62** *via* Rh/**L12**-catalyzed double bond isomerization.

Based on a series of control experiments, a plausible mechanism was proposed. Initially, $[Rh(C_2H_4)_2Cl]_2$ reacted with $AgSbF_6$ and **L12** to generate the cationic catalyst [Rh**L12**]SbF_6, which then coordinated with (*Sa*)-**60** to generate intermediate **63**. The subsequent cyclometallation formed intermediate **63**, which then underwent allylic isomerization to produce rhodiabicycloheptene **65**. Reductive elimination delivered the [4+2] cycloadduct **66** and regenerated [Rh**L11**]$^+$ (Path a). From **66**, the *in situ* formed [Rh]–H species promoted isomerization of the C=C bond *via* sequential hydrometallation and β-H elimination to afford **61** as the final product. Meanwhile, the enantiomeric (*Ra*)-**60** coordinated with [Rh**L11**]$^+$ and underwent oxidative addition to generate allyl-Rh-hydride intermediate **69**. The reductive elimination of **69** and ligand dissociation then produced tetraene products **62** (path b). It should be noted that (*Sa*)-**60** could also proceed through path b slowly to give **62** in a reduced yield, thus revealing the delicate balance between cyclization and isomerization processes.

Based on the above achievements, the Ma group realized the first Rh-catalyzed dynamic kinetic resolution (DKR) of racemic axially chiral allene-1,3-dienes through the intramolecular [4+2] cycloaddition paradigm, establishing a powerful approach for the construction of enantiopure 5/6-bicyclic scaffolds (Scheme 19).[78] By the catalysis of $[Rh(coe)_2Cl]_2$/AgOTs/**L12** in isopropanol at 80 °C, a wide range of *cis*-5,6-fused bicyclic products **72** were obtained with high yields and excellent enantioselectivities (up to 84% yield and >99% ee) directly from racemic allene-1,3-dienes **71**. The key for the success of

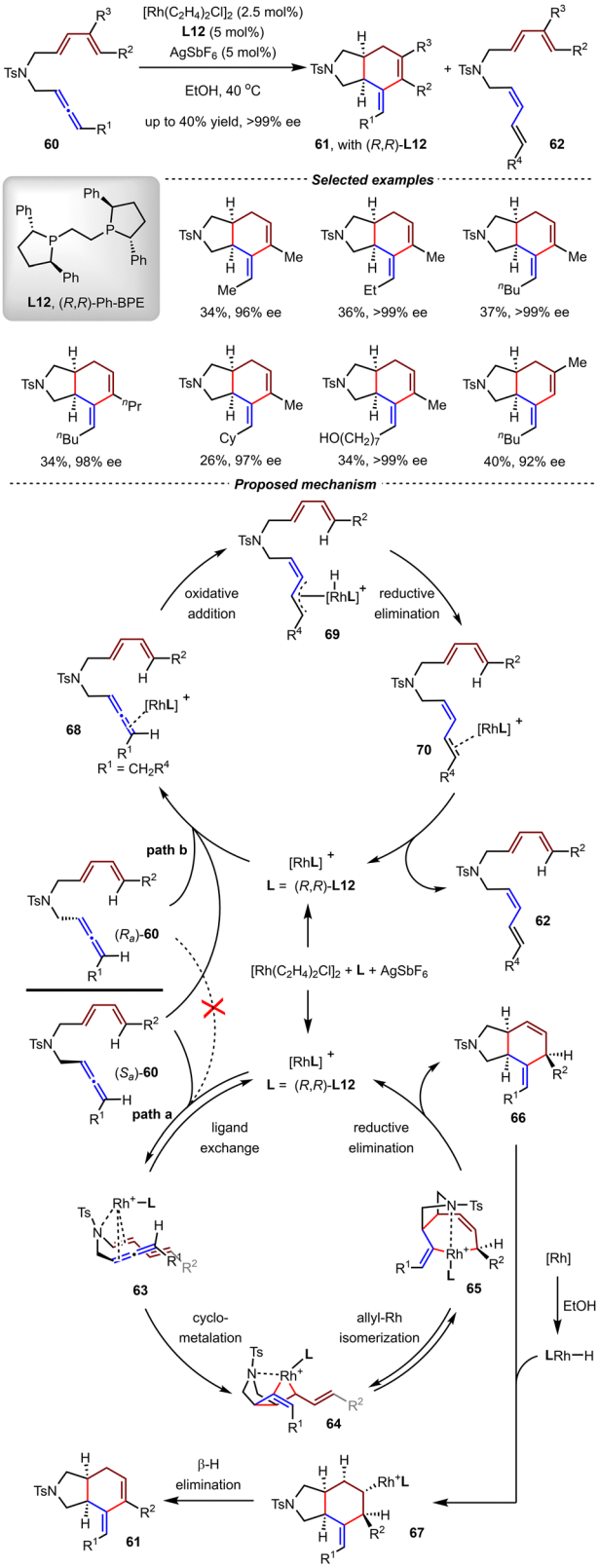

Scheme 18 Rh(I)/Ph-BPE-catalyzed kinetic resolution of racemic 1,3-disubstituted allene-1,3-dienes.

this transformation was the judicious selection of Malphos **L13** as the chiral ligand. Combined mechanistic experiments and

This journal is © The Royal Society of Chemistry 2026

Open Access Article. Published on 13 2026. Downloaded on 08/05/26 22:54:22.
This article is licensed under a Creative Commons Attribution 3.0 Unported Licence.

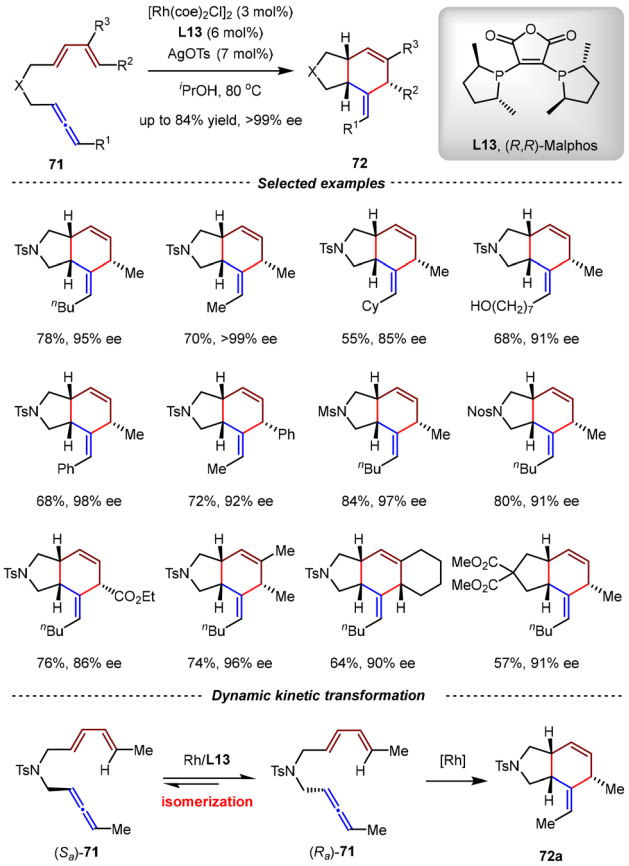

Scheme 19 Rh(I)/Malphos-catalyzed dynamic kinetic resolution (DKR) of racemic allene-1,3-dienes *via* the intramolecular [4+2] cycloaddition.

DFT calculations revealed that the Rh/**L13** complex could facilitate the isomerization of (*Sa*)-**71** to (*Ra*)-**71** and then stereoselectively promoted the subsequent [4+2] cycloaddition of (*Ra*)-**71**. It was proposed that the racemization of **71** was not caused by the *in situ* generated rhodium hydride species, but by the coordination with Rh/**L13** followed by the subsequent C–H oxidative addition and reductive elimination. Compared with the ability of (*R*,*R*)-Ph-BPE **L12** to promote the isomerization of allenes to 1,3-dienes, the distinctive reactivity of **L13** demonstrated the striking ligand effect.

2.2. Pd-catalyzed [4+2] cycloadditions

Despite remarkable achievements realized by Rh(I) complexes in intramolecular [4+2] cycloadditions of allene-1,3-dienes, the intermolecular version of these transformations remained elusive. In 1997, Murakami and Ito *et al.* developed the palladium-catalyzed intermolecular [4+2] cycloadditions of 1,3-dienes and vinylallenes (Scheme 20).[79] Using $Pd(PPh_3)_4$ as the catalyst, vinylallenes reacted as diene components to contribute a four-carbon unit in [4+2] cycloadditions with 1,3-dienes at room temperature, delivering substituted cyclohexene derivatives with high yields and diastereoselectivities. Notably, the reaction between isoprene and vinylallene afforded a pair of isomers in 97% yield with 71 : 29 regioselectivity. In a proposed mechanism, the reaction began with the [4+1] type of oxidative

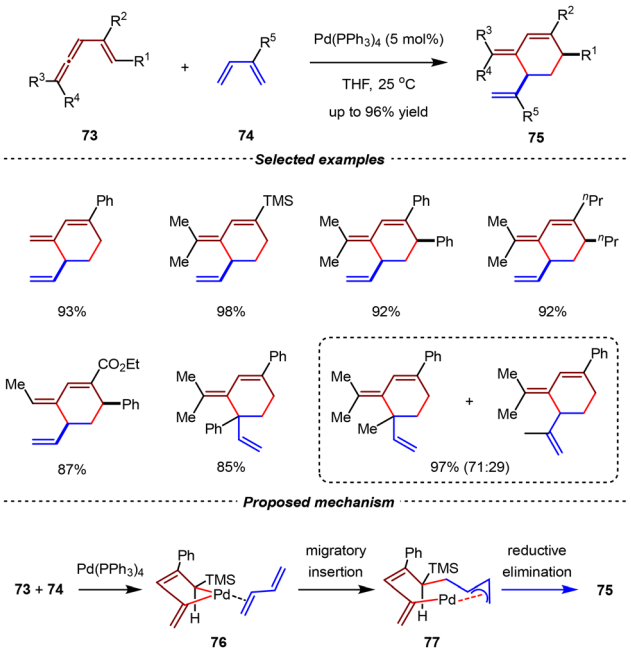

Scheme 20 $Pd(PPh_3)_4$-catalyzed intermolecular [4+2] cycloadditions of vinylallenes and 1,3-dienes.

cyclometallation between vinylallenes **73** and $Pd(PPh_3)_4$, generating the five-membered bent palladacycle intermediate **76** in an s-*trans* coordination geometry. Subsequently, the π-allylpalladium intermediate **77** was formed *via* migratory insertion of the 1,3-diene into the palladacycle, leading to **77**, which subsequently underwent reductive elimination to give **75**. This study significantly advanced the development of transition metal-catalyzed [4+2] cycloadditions, providing an unconventional approach for constructing structurally diverse six-membered carbocycles.

In 2000, the Ito group achieved a breakthrough in the development of a catalytic asymmetric variant of this transformation (Scheme 21).[80] After evaluation of various ferrocene-derived monophosphine ligands, the combination of $Pd_2(dba)_3$·

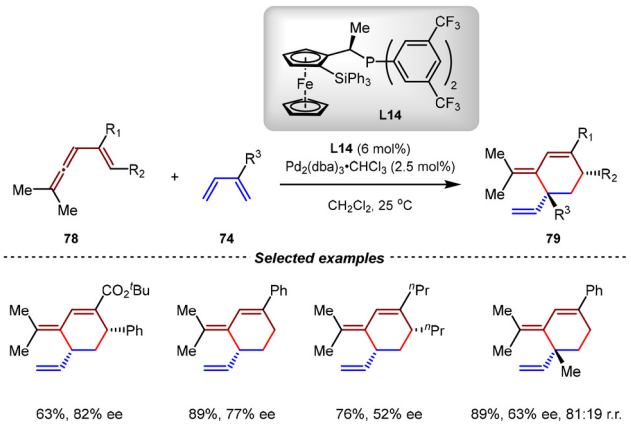

Scheme 21 Pd(0)-catalyzed asymmetric intermolecular [4+2] cycloadditions of vinylallenes and 1,3-dienes.

Open Access Article. Published on 13 2026. Downloaded on 08/05/26 22:54:22.
This article is licensed under a Creative Commons Attribution 3.0 Unported Licence.

$CHCl_3$ with **L14** was found to be effective, facilitating the intermolecular cycloadditions of vinylallenes **78** and 1,3-dienes **74** in dichloromethane under mild reaction conditions. In these reactions, vinylallenes bearing ester, phenyl, and alkyl groups all reacted smoothly with 1,3-butadienes to afford the desired products in high yields, albeit with moderate enantioselectivities (up to 82% ee).

2-Carboalkoxy-1,3-butadienes (2-CBDs) **80** are electron-deficient dienes which are facile to self-dimerization under mild conditions.[81] Recently, the Cai group employed readily available Morita–Baylis–Hillman (MBH) carbonates **82** as precursors of 2-CBDs. Through the Pd(0)-catalyzed oxidative addition followed by the β-H elimination, 2-CBD intermediates were generated *in situ* and their dimerization was suppressed by coordination with Pd(0) (Scheme 22).[82] Using **L15** as the chiral ligand, the asymmetric [4+2] cycloaddition between MBH carbonates **84** and 1,3-enynes **85** went on smoothly, giving 1,4-cyclohexadiene derivatives **86** bearing aryl- and alkyl-substituents with excellent yields and high enantioselectivities (up to 98% yield, 96% ee). By DFT calculations, it was proposed that the *in situ* generated 2-CBD coordinated with Pd/**L15**, giving intermediate **87**, which then underwent [4+4+1] oxidative cyclometallation with 1,3-enyne **85** to afford Pd(II) species **88**. Owing to the *trans*-configuration of the olefin moiety in **88**, allylic isomerization and rotation steps should occur before reductive elimination, thus delivering intermediate **90**. From **90**, the reductive elimination afforded the final product **86** in a chemo-, regio-, and enantioselective manner.

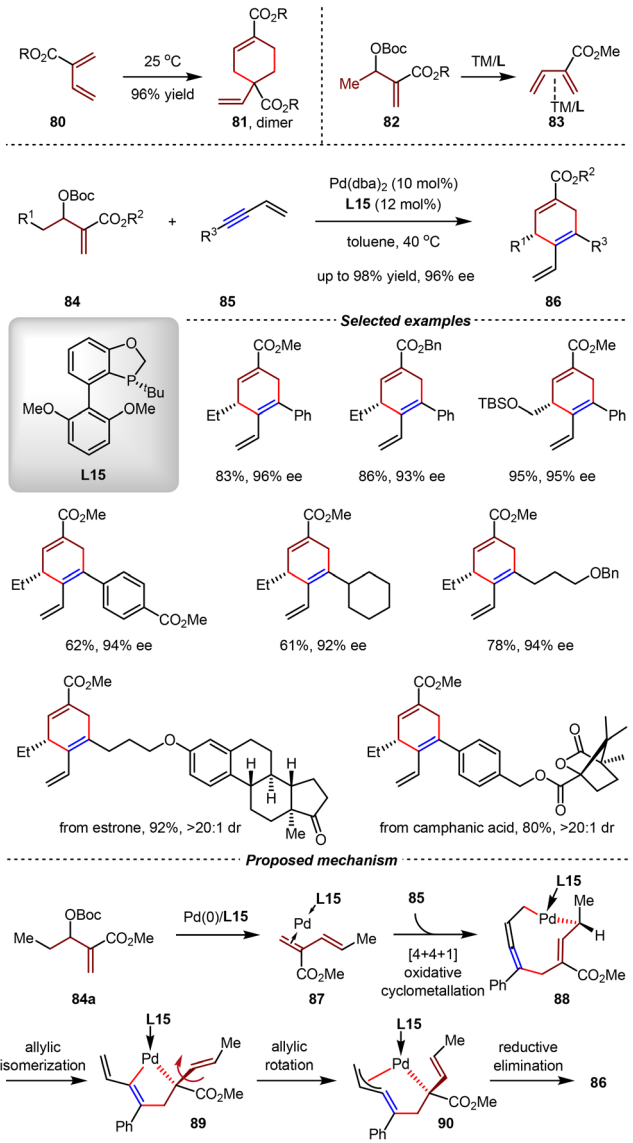

Scheme 22 Pd(0)-catalyzed asymmetric [4+2] cycloadditions of Morita–Baylis–Hillman carbonates and 1,3-enynes.

2.3. Ir-catalyzed [4+2] cycloadditions

In 2002, the Shibata group demonstrated that the iridium complex had sufficient catalytic activity to promote [4+2] cycloadditions of unactivated diene-ynes (Scheme 23).[83] The catalytic enantioselective intramolecular [4+2] cycloadditions of diene-ynes **91** were realized by $[Ir(cod)Cl]_2$ and BDPP **L16**, enabling the synthesis of chiral cyclohexa-1,4-dienes **92** with high yields and enantioselectivities (up to 73% yield, 98% ee). This study illustrated the versatility of iridium catalysis in asymmetric cycloadditions. However, only aryl-substituted diene-yne substrates were evaluated, leaving alkyl-substituted variants unexplored.

2.4. Ru-catalyzed [4+2] cycloadditions

In 2000, the Trost group realized the $RuCp(MeCN)_3FP_6$-catalyzed intramolecular [4+2] cycloadditions of yne-enones, giving bicyclic 4*H*-pyrans with high yields. According to the proposed mechanism, three vacant coordination sites were required on the Ru(II) center, thus making the use of a chiral cyclopentadienyl (Cp) ligand a promising strategy to achieve good enantioselectivity control.[84] In 2015, the Cramer group developed an efficient route for the synthesis of various cationic CpRu(II) complexes bearing chiral ligands and then evaluated these complexes in intramolecular [4+2] cycloadditions of yne-enones.[85,86] Using **94** as the catalyst at −20 °C, the intramolecular formal [4+2] cycloadditions of yne-enones **93** proceeded efficiently to deliver 2*H*-pyran derivatives **95** with high yields and excellent enantioselectivities (up to 95% yield, 98% ee)

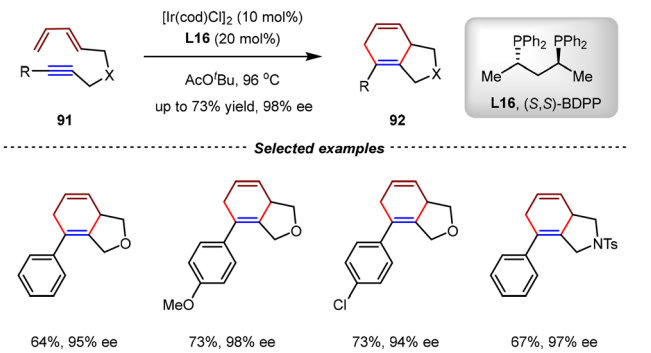

Scheme 23 Ir(I)/BDPP-catalyzed asymmetric intramolecular [4+2] cycloaddition of diene-ynes.

This journal is © The Royal Society of Chemistry 2026

Open Access Article. Published on 13 2026. Downloaded on 08/05/26 22:54:22.
This article is licensed under a Creative Commons Attribution 3.0 Unported Licence.

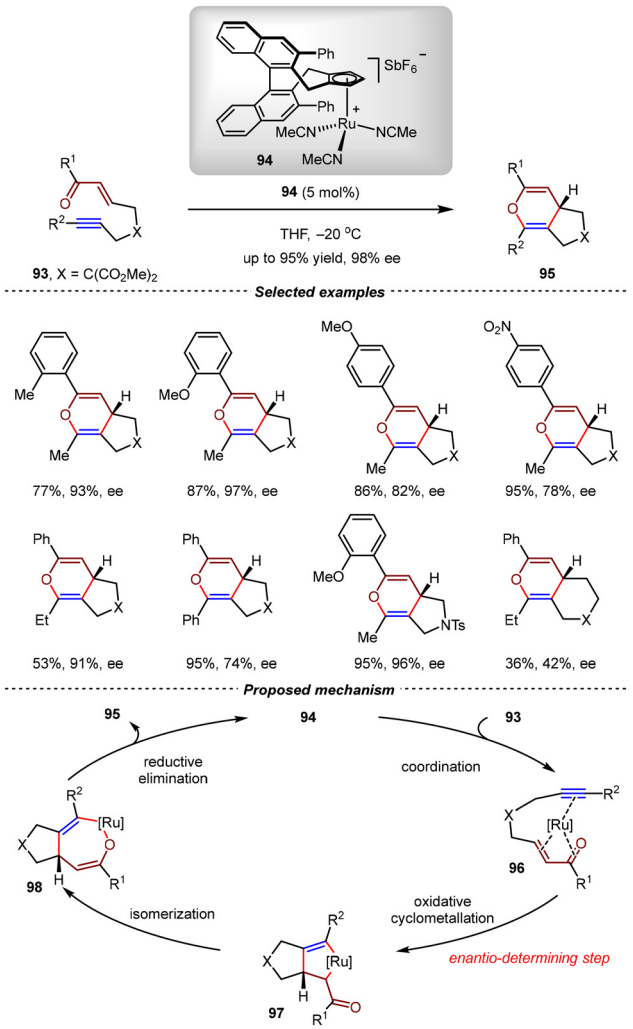

Scheme 24 Ruthenium (II)-catalyzed asymmetric intramolecular [4+2] cycloadditions of yne-enones.

(Scheme 24). In a proposed mechanism, the CpRu(II) complex **94** initially coordinated with yne-enone **93** to generate intermediate **96**, which then underwent oxidative cyclometallation, allylic isomerization, and reductive elimination to afford **95** as the final product. Notably, the enantioselectivity was determined in the oxidative cyclometallation step.

2.5. Ni-catalyzed [4+2] cycloadditions

The Ni(0)-catalyzed cycloadditions of 1,3-dienes represent one of the earliest and most important transition metal-catalyzed C–C bond-forming reactions.[87–89] Since the early 1960s, the Wilke group systematically investigated the cyclodimerization of 1,3-butadiene.[90–92] In 1974, the Garrat group developed the intermolecular [4+2] cycloaddition between two different 1.3-dienes.[93] In the presence of a nickel catalyst [$Ni(acac)_2$, Et_3Al, PPh_3], the cross-[4+2] cycloaddition of 1,3-butadiene **99** with methyl sorbate **100** gave a pair of diastereomeric formal inverse-electron-demand [4+2] cycloadducts **102** and **102′** in 90% yield with 2 : 1 dr. It should be noted that under thermal conditions, methyl sorbate **100** acted as the diene component,

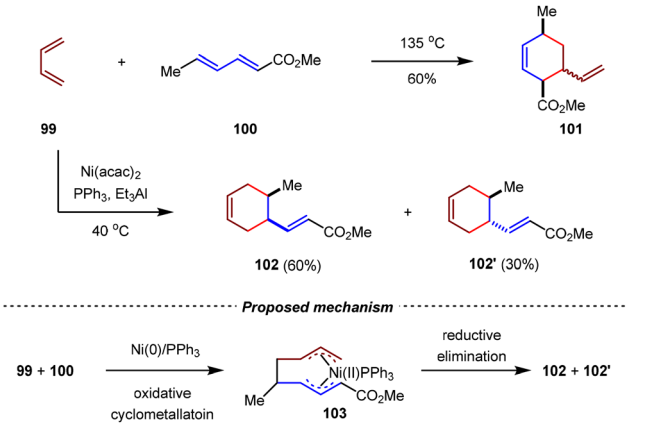

Scheme 25 Ni(0)/PPh_3-catalyzed cross-[4+2] cycloadditions of 1,3-butadiene with methyl sorbate.

while 1,3-butadiene **99** served as the dienophile to afford normal-electron-demand cycloadduct **101** exclusively. A plausible mechanism for the Ni(0)-catalyzed [4+2] cycloaddition is illustrated in Scheme 25. The oxidative cyclometallation of **99** and **100** with the Ni(0)/PPh_3 catalyst afforded the key bis(η^3-allyl)nickel(II) intermediate **103**, which then underwent reductive elimination to produce the cycloaddition product. These results clearly indicated that the transition metal catalysis could not only accelerate the reaction rate but also change the inherent periselectivity in [4+2] cycloadditions of unsaturated hydrocarbons.

The first asymmetric Ni(0)-catalyzed intermolecular [4+2] cycloaddition of 1,3-dienes was reported by the Mortreux group in 1994.[94] By the catalysis of $Ni(cod)_2$ and bis(aminophosphine) ligand **L17** in toluene at 80 °C, 1,3-butadiene **99** underwent [4+2] dimerization to generate 4-vinylcyclohexene **104** in 80% yield but with only 6% ee. In this reaction, 1,5-cyclooctadiene **105** by [4+4] co-dimerization of **99** was obtained as the main side product in 20% yield (Scheme 26). In 1995, the same group reported the Ni(0)-catalyzed cross-[4+2] cycloaddition of methyl penta-2,4-dienoate **95** with 1,3-butadiene **99**.[95] Using $Ni(cod)_2$/(*R*)-BINAP **L3** as the catalyst, the cross-[4+2] cycloadduct **107** was produced in 15% yield and 5% ee, and the co-dimerization

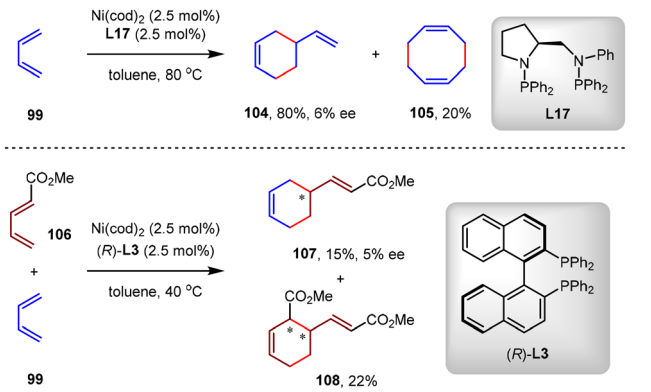

Scheme 26 Ni(0)-catalyzed asymmetric [4+2] cycloadditions of 1,3-dienes.

Open Access Article. Published on 13 2026. Downloaded on 08/05/26 22:54:22.
This article is licensed under a Creative Commons Attribution 3.0 Unported Licence.

product **108** from **106** was generated in 22% yield (Scheme 26). The poor results in these two reactions demonstrated the substantial challenge in controlling both the chemoselectivity and enantioselectivity concurrently in Ni(0)-catalyzed asymmetric [4+2] cycloadditions of 1,3-dienes.

A breakthrough in this research field was achieved by the Chen group in 2022.[96] Using $Ni(cod)_2$ as the catalyst and chiral N-heterocyclic carbene (NHC) **L18** as the ligand, a wide range of unnatural cyclic monoterpene derivatives bearing quaternary carbon stereocenters were obtained in high yields and enantioselectivities (up to 98% yield, 97% ee) from isoprene and heterocycles (Scheme 27). By this method, various heterocycles, such as purines, adenines, and imidazoles, could be incorporated into the terpene skeleton. Mechanistic studies and DFT calculations revealed that this atom-economic reaction proceeded through the enantioselective [4+2] dimerization of isoprene followed by a sequential C–H alkylation of the heterocycle pathway. As shown in Scheme 27, the oxidative cyclometallation of isoprene with the Ni(0) catalyst proceeded through intermediate **111**, giving the five-membered nickelacycle intermediate **112**. By coordination with another isoprene, intermediate **113** was generated and underwent migratory insertion through transition state **114**, thus affording seven-membered nickelacycle **115**. Subsequently, reductive elimination of the Ni(II) species **115** produced the [4+2] cycloadduct **116** bearing a quaternary carbon center. Parallelly, the nickel–hydride intermediate **118** was formed from the heterocycle substrate *via* C–H activation with the Ni(0) catalyst. From **116** and **118**, the sequential coordination followed by the migratory insertion and reductive elimination produced the final product **110** and regenerated the Ni(0) catalyst. Notably, the key for the success of this transformation was the judicious selection of a bulky C_2-symmetric NHC **L18** to realize the chemo-, regio-, and enantioselectivity.

In addition to the Pd(0)-catalyzed [4+2] cycloadditions of MBH carbonates with 1,3-enynes, the Cai group also reported the asymmetric formal inverse-electron-demand [4+2] cycloaddition of MBH carbonates **121** with 1,3-dienes **122** by the catalysis of Ni(0)/**L19** (Scheme 28).[82] A wide range of *para*-substituted cyclohexenes **123** were obtained in high yields with excellent chemo-, regio- and stereoselectivities (up to 94% yield, 99% ee, >20 : 1 rr). Intriguingly, this catalytic system could be applied to [4+2] cycloadditions between two electron-deficient dienes, which was an unsolved reaction mode in organic synthesis before this study. In analogous to conventional Diels–Alder reactions, these reactions demonstrated remarkable stereospecificity. When internal (*E*,*Z*)-1,3-dienes were used, the reaction occurred on the double bond adjacent to the alkyl group, affording *cis*-cycloadducts. (*E*,*E*)-1,3-diene was also compatible, and the *trans*-cycloadduct was produced. Owing to the mild and redox-neutral conditions, a wide range of conjugated trienes and air/light-sensitive tetraenes were tolerated. The utilization of these reactions in complex molecule synthesis was demonstrated by the three-step synthesis of (+)-juvabione and (+)-epijuvabione.[82] By DFT calculations, it was proposed that the [4+2] cycloaddition went through a pathway involving

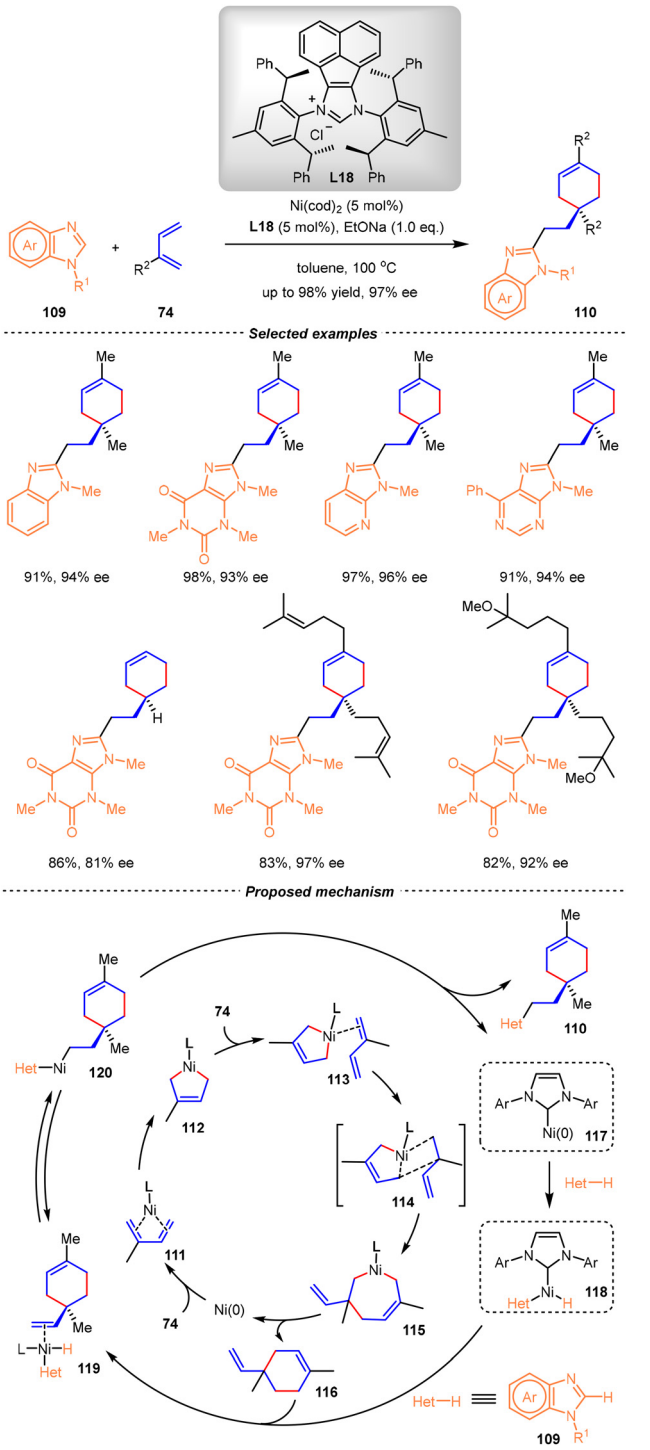

Scheme 27 Ni(0)/NHC-catalyzed asymmetric heteroarylative cyclotelomerization of isoprene.

[4+4+1] oxidative cyclometallation, allylic isomerization, and reductive elimination steps.

2.6. Fe-catalyzed [4+2] cycloadditions

The applications of iron catalysts have attracted increasing attention in recent years, owing to their abundance, low price, and unique reactivities to promote synthetic transformations

This journal is © The Royal Society of Chemistry 2026

Open Access Article. Published on 13 2026. Downloaded on 08/05/26 22:54:22.
This article is licensed under a Creative Commons Attribution 3.0 Unported Licence.

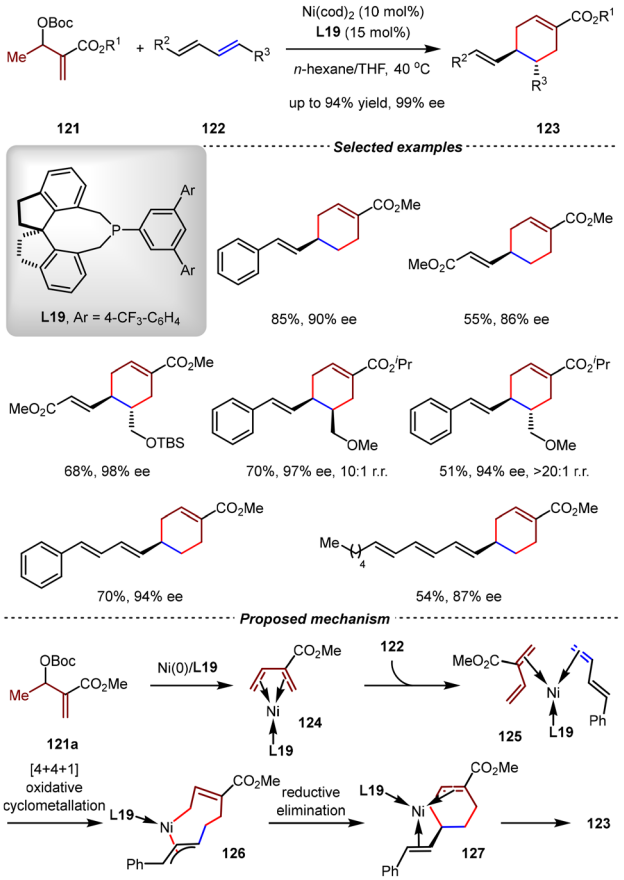

Scheme 28 Ni(0)-catalyzed [4+2] cycloadditions of Morita–Baylis–Hillman carbonates with 1,3-dienes.

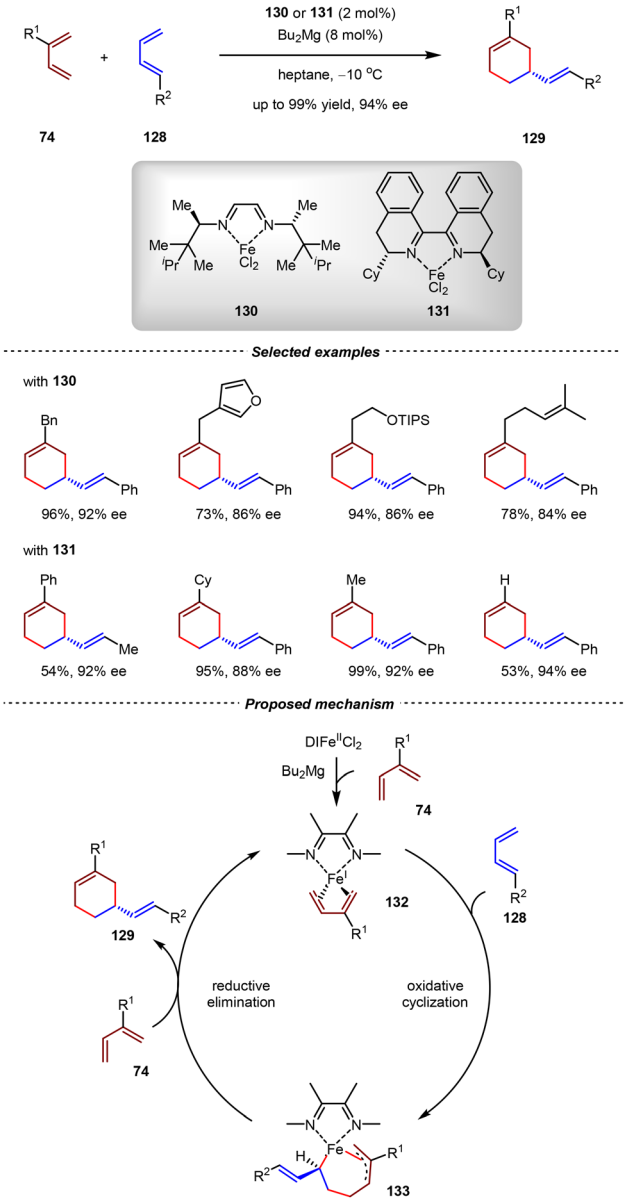

Scheme 29 Fe(I)/α-diimine-catalyzed asymmetric cross-[4+2] cycloadditions of unactivated 1,3-dienes.

that are otherwise challenging to be achieved by other catalytic systems.[97–100] In 2020, the Cramer group realized a catalytic asymmetric cross-[4+4] cycloaddition between two different unactivated 1,3-dienes to form substituted cyclooctadienes by a chiral α-diimine iron complex.[101] Based on this study, they developed a new chiral α-diimine iron catalyst that enabled the cross-[4+2] cycloadditions between unactivated 1-substituted 1,3-dienes and 2-substituted 1,3-dienes in a regioselective and enantioselective manner (Scheme 29).[102] Using the iron complex **130** or **131** as the catalyst, a series of alkyl- and aryl-substituted *meta*-substituted vinyl cyclohexene derivatives **129** were obtained in high yields with excellent enantioselectivities (up to 99% yield, 94% ee). It should be noted that by conventional Diels–Alder reactions, only *para*- and *ortho*-substituted cyclohexene adducts could be produced, thus demonstrating the complementary advantage of the iron catalysis.

In a proposed reaction mechanism, the Fe(II) complex was initially reduced by $MgBu_2$ to generate the Fe(I) catalyst, which then coordinated with 1,3-diene **74** to form the catalytically active species **132**. Then, the oxidative cyclometallation between intermediate **132** and 1-substituted 1,3-diene **128** led to the formation of seven-membered ferracycle **133** regioselectively. Finally, a reductive elimination formed 1,3-substituted vinyl cyclohexene **129** and regenerated **132**. This study unambiguously showcased that the main skeletons of α-diimine ligands played an important role in controlling the periselectivity in cycloaddition.

2.7. Co-catalyzed [4+2] cycloadditions

As an important type of earth-abundant transition metal in organic synthesis, the cobalt catalysts demonstrated sufficient ability to promote cycloadditions of unsaturated hydrocarbons.[103–108] The Hilt group has systematically investigated the Co(I)-catalyzed [4+2] cycloadditions between unactivated 1,3-dienes and alkynes.[109–111] In these reactions, various functionalities were compatible on the 1,3-diene and alkyne moieties with various substitution patterns.[103–105] However, catalytic asymmetric variants of these transformations were

Open Access Article. Published on 13 2026. Downloaded on 08/05/26 22:54:22.
This article is licensed under a Creative Commons Attribution 3.0 Unported Licence.

ignored for many years. In 2023, the Rajanbabu group reported the first cobalt-catalyzed enantioselective [4+2] cycloadditions between 1,3-dienes and internal alkynes (Scheme 30).[112] In the presence of catalytic amounts of $CoBr_2$/BenzP*(**L20**) and zinc powder, highly functionalized 1,4-cyclohexadienes **135** were obtained in high yields and enantioselectivities (up to 82% yield, 99% ee) from 1-substituted 1,3-dienes **128** and electron-deficient alkynes **134**. Notably, unsymmetric 1,3-dienes and alkynes were compatible in these reactions, leading to excellent regioselectivities in most cases. In control experiments, when the isolated [Co(I)Br**L20**]$_2$ complex was used as the catalyst, no [4+2] cycloadduct was observed. In contrast, the combination of the same complex with NaBARF led to the formation of the desired [4+2] product with 100% conversion, indicating the key role of the cationic properties of the situ generated [Co**L20**]$^+$[BARF]$^-$ catalyst.

In a possible mechanism, the Co(I)/**L20** complex was initially generated from $CoBr_2$ and **L20** by reduction with zinc. Then, it coordinated with the 1,3-diene and alkyne substrates to form intermediate **137**, which underwent the turn-over limiting

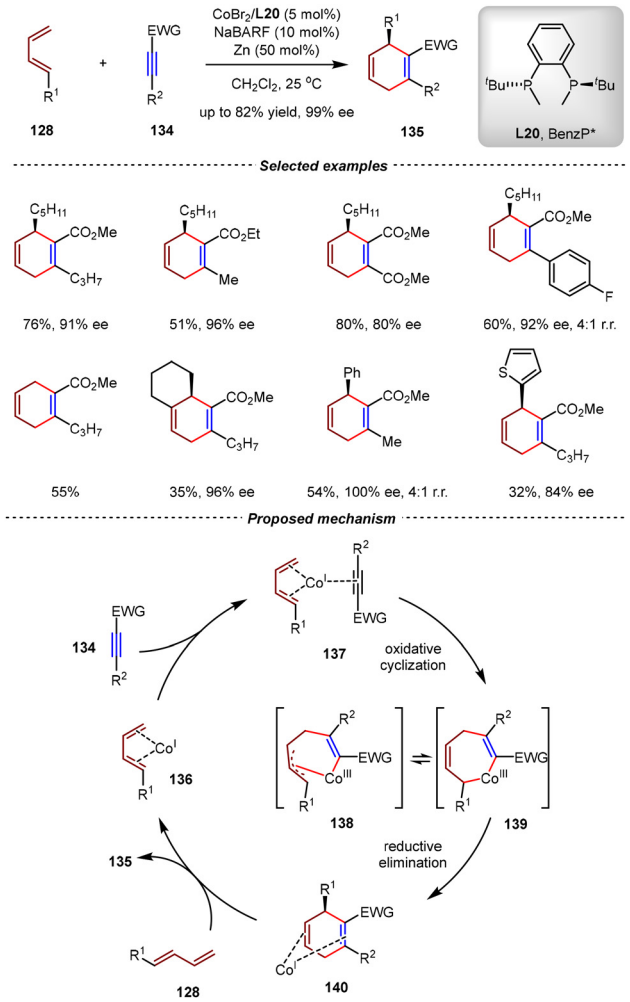

Scheme 30 Co(I)/BenzP*-catalyzed asymmetric [4+2] cycloadditions of 1,3-dienes and alkynes.

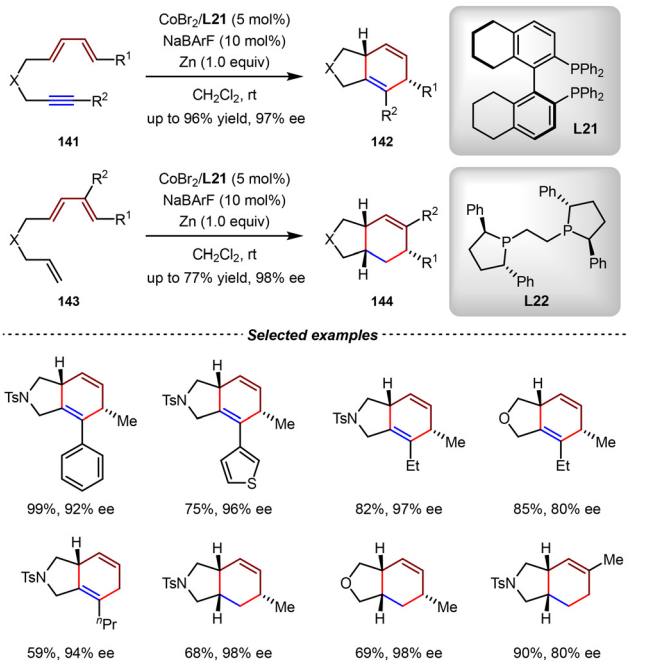

Scheme 31 Co(I)-catalyzed intramolecular [4+2] cycloaddition reactions of unactivated diene-ynes and trienes.

oxidative cyclometallation to generate [Co(III)]-metallacycle **139**. The subsequent rapid reductive elimination formed the second C–C bond, yielding the final product **135** and regenerating the active catalyst. Remarkably, the utilization of the (*R*)-*t*Bu-PHOX ligand instead of **L20** enabled asymmetric [2+2] cycloadditions between 1,3-dienes and alkynes, further highlighting the crucial role of chiral ligands in controlling both the regioselectivity and chemoselectivity.

Recently, the Rajanbabu group reported the asymmetric cobalt-catalyzed intramolecular [4+2]-cycloadditions of unactivated diene-ynes **141** and trienes **143** (Scheme 31).[113] In the presence of catalytic amounts of $CoBr_2$/(*S*)-H_8-BINAP (**L21**) and zinc powder, a series of 5/6-bicyclic products **142** were obtained as single diastereoisomers with excellent yields and enantioselectivities (up to 96% yield, 93% ee) from diene-ynes **141**. When the $CoBr_2$/**L22** complex was used, trienes **143** underwent highly selective [4+2] cycloaddition, affording the fused 5,6-bicyclic products **144** rather than the intramolecular [2+2] cycloaddition products. Notably, the appropriate ligand was proved to be crucial for controlling the periselectivity of the [2+2] cycloaddition reaction.

3. Enantioselective [4+2] cycloadditions *via* the LUMO activation of π-acids

In the past two decades, homogenous gold(I) catalysis has showcased its powerful ability in the construction of carbon–carbon bonds and carbon–heteroatom bonds.[44–50,114–117] According to the Dewar–Chatt–Duncanson (DCD) bonding

This journal is © The Royal Society of Chemistry 2026

Open Access Article. Published on 13 2026. Downloaded on 08/05/26 22:54:22.
This article is licensed under a Creative Commons Attribution 3.0 Unported Licence.

model, the Au(I) metal can coordinate with the alkene or alkyne ligand, forming a strong dative σ bond by overlap of the π orbital of the ligand with the low-lying empty orbital of the Au(I) metal center. Meanwhile, the Au(I) center backdonates the electron density from its filled d orbital into the π* antibonding orbital of the alkene/alkyne ligand. Since this backdonation is relatively weak, the interaction between the metal center and the ligand is dominated by the ligand-to-metal σ electron-donation, therefore making the alkene or alkyne ligand electrophilic.[42] Based on this unique π-acid activation mode, significant advancements have been achieved in Au(I)-catalyzed formal [4+2] cycloadditions.

In 2009, the Toste group reported a striking example of ligand-controlled gold(I)-catalyzed intramolecular [4+2] or [4+3] cycloadditions of allene-1,3-dienes with high selectivity (Scheme 32).[118] Using di-*tert*-butylbiphenylphosphine **L23** as the ligand, the allene-1,3-diene substrates underwent intramolecular [4+3] cyclization, affording 5/7 bicyclic adducts **146** exclusively. Intriguingly, changing the ligand from **L23** to triarylphosphite ligand **L24** altered the reaction pathway completely, leading to [4+2] *trans*-adducts **147** with up to 92% yield. In a proposed mechanism, the Au(I) catalyst coordinated with the allene moiety and then induced the intramolecular cyclization with the 1,3-diene part by the π-acid activation mode. It was hypothesized that the electron-rich σ-donor ligand **L23** preferentially stabilized intermediates **148** and **149**, thereby favoring [4+3] cycloadduct formation over path a. In contrast, the π-acceptor ligand **L24** preferentially stabilized intermediates **150** and **151**, thereby promoting the reaction to proceed through path b to form the [4+2] cycloadduct. This study established a fundamental framework to control the chemoselectivity in Au(I)-catalyzed cycloaddition reactions by ligand variations.

Almost at the same time, the asymmetric gold(I)-catalyzed intramolecular asymmetric cycloaddition of allene-1,3-dienes was reported by the Mascareñas group (Scheme 33).[119] Using phosphoramidite **L25** with C3/C3' substituents on the BINOL skeleton as the chiral ligand, the intramolecular [4+2] cycloaddition of nitrogen-tethered allene-1,3-dienes **152** enabled the synthesis of *trans*-5,6- and 6,6-fused bicyclic products **153** with up to 93% yield and 97% ee. By experimental investigations and DFT calculations, a plausible mechanism was proposed. Initially, the Au(I)/**L25** catalyst coordinated and activated the allene unit by π-acid activation to form gold-allyl intermediate **155**, which then underwent intramolecular and concerted *exo*-like [4+3] cycloaddition with the 1,3-diene moiety to generate cycloheptenyl Au-carbene intermediate **156**. Subsequently, the ring contraction of **156** *via* the 1,2-alkyl shift delivered the final [4+2] cycloadduct **157** and regenerated the Au(I) catalyst. According to this mechanism, both the formal [4+3] and [4+2] cycloaddition reaction pathways shown in Scheme 32 shared the same [4C(4π) + 3C(2π)] cycloaddition step between the diene moiety and the Au(I)-allyl cation intermediate.

In 2010, the Toste group also reported an enantioselective Au(I)-catalyzed intramolecular [4+2] cycloaddition of carbon-tethered allene-1,3-dienes (Scheme 34).[120] Using the C_3-symmetric

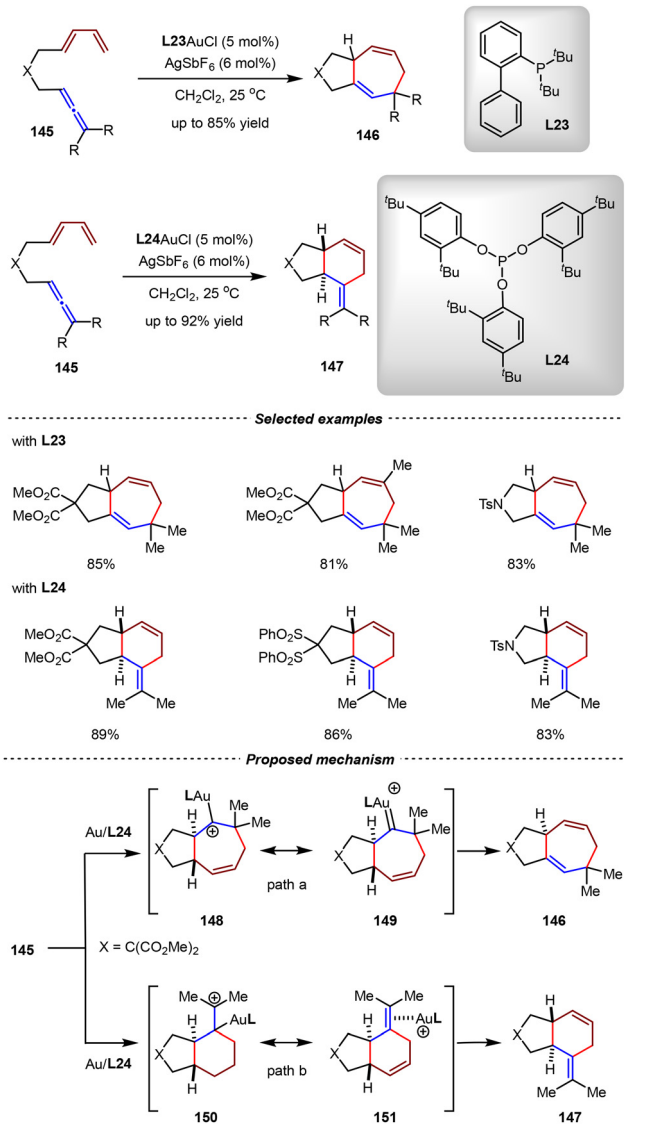

Scheme 32 Au(I)-catalyzed intramolecular [4+3] and [4+2] cycloadditions of allene-dienes.

monodentate phosphite **L26** as the chiral ligand, a series of enantioenriched *trans*-hexahydroindenes were selectively accessible from allene-1,3-dienes by gold(I) catalysis. This study together with Mascareñas's discovery demonstrated that chiral monodentate phosphorus-based ligands were suitable in asymmetric Au catalysis despite the linear geometry of Au(I) complexes.

The first Au(I)-catalyzed asymmetric intermolecular [4+2] cycloadditions were reported by the Mascareñas group in 2012.[121] In the presence of catalytic amounts of Au(I) complex **163** and $AgNTf_2$, the intermolecular [4+2] cycloadditions between allenamides and 1,3-dienes went on smoothly, affording optical active cyclohexene products with excellent yields and enantioselectivities (up to 88% yield, >99% ee, Scheme 35). The key for the success of these reactions was the utilization of an axially chiral N-heterocyclic carbene (NHC) ligand featuring a triazole scaffold. The X-ray structure demonstrated that Au(I)

Open Access Article. Published on 13 2026. Downloaded on 08/05/26 22:54:22.
This article is licensed under a Creative Commons Attribution 3.0 Unported Licence.

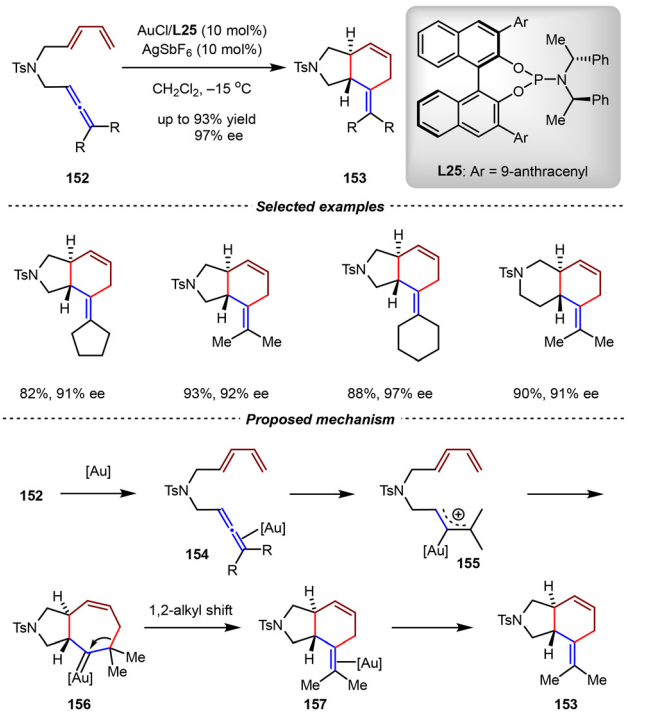

Scheme 33 Au(I)/phosphoramidite-catalyzed asymmetric intramolecular [4+2] cycloadditions of nitrogen-tethered allene-dienes.

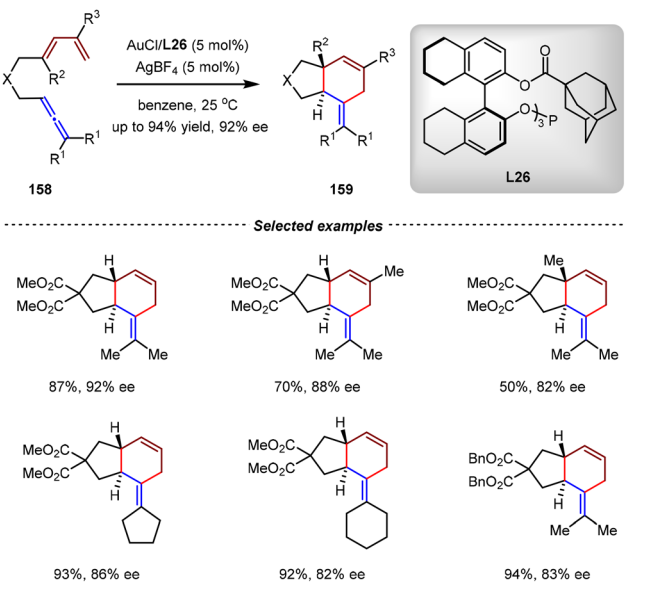

Scheme 34 Au(I)/C_3-symmetric phosphite-catalyzed asymmetric intramolecular [4+2] cycloadditions of allene-dienes.

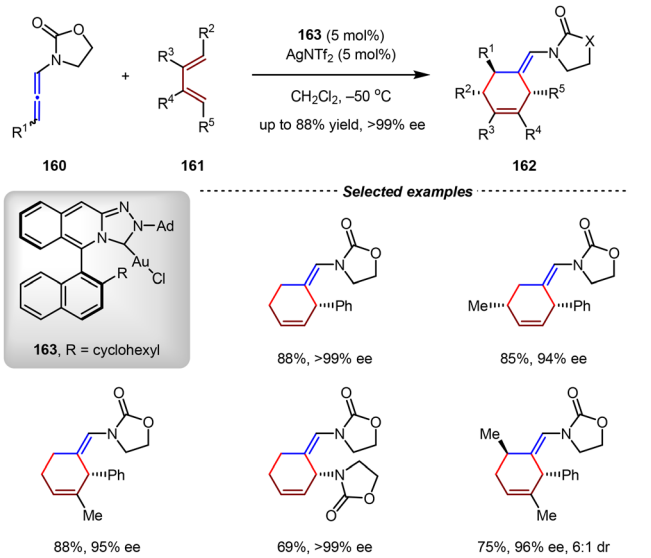

Scheme 35 Au(I)/NHC-catalyzed asymmetric intermolecular [4+2] cycloadditions of allenamides and 1,3-dienes.

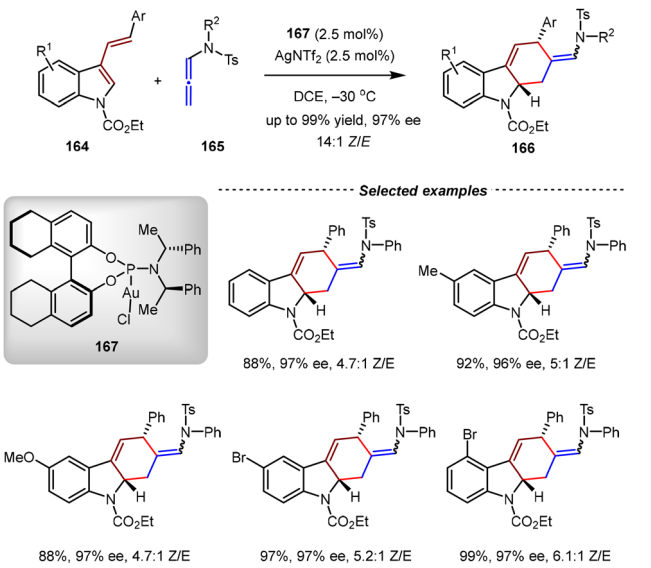

Scheme 36 Au(I)/phosphoramidite-catalyzed asymmetric intermolecular [4+2] cycloadditions of 3-styrylindoles and *N*-allenamides.

complex **163** had a high percentage of buried volume value (V_{bur} = 46.2%) around the Au(I) center, indicating the significant steric hinderance of the NHC ligand.

In 2015, the Zhang group disclosed the enantioselective [4+2] cycloadditions of 3-styrylindoles and *N*-allenamides catalyzed by an Au(I)/chiral phosphoramidite complex (Scheme 36).[122] By this method, a wide range of optically active tetrahydrocarbazoles were obtained with high yields and enantioselectivities (up to 99% yield, 97% ee). DFT calculations revealed that an Au(I)-allyl cation species was generated from the *N*-allenamide substrate by the activation of the Au(I) catalyst. Then, a stepwise [4+2] cycloaddition occurred with the 3-styrylindole substrate, in which the C2-position of the indole moiety served as the nucleophilic site due to the electron-withdrawing character of the *N*-CO_2Et group.

In 2017, the Rossi group reported the Au(I)-catalyzed asymmetric intermolecular [4+2] cycloadditions between 3-substituted 2-vinylindoles and *N*-allenamides (Scheme 37).[123] Using DTBM-Segphos **L27** as the chiral ligand, dearomative

This journal is © The Royal Society of Chemistry 2026

Open Access Article. Published on 13 2026. Downloaded on 08/05/26 22:54:22.
This article is licensed under a Creative Commons Attribution 3.0 Unported Licence.

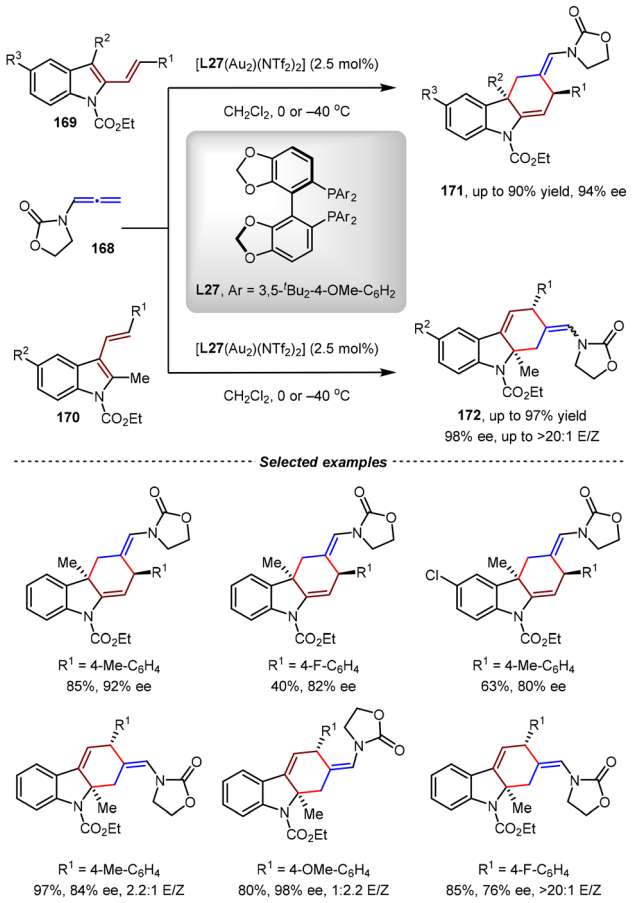

Scheme 37 Au(I)/DTBM-Segphos-catalyzed asymmetric dearomative [4+2] cycloadditions of 3/2-substituted 2/3-vinylindoles and *N*-allenamides.

tetrahydrocarbazoles bearing a quaternary stereogenic center at the C3-position were obtained in good yields and enantioselectivities (up to 90% yield, 94% ee). Encouraged by these results, isomeric 2-methyl-3-vinylindoles were also evaluated, and the corresponding tetrahydrocarbazoles bearing a quaternary stereogenic center at the C_2-position were produced with excellent yields and enantioselectivities (up to 97% yield, 98% ee, >20 : 1 E/Z).

In a proposed mechanism (Scheme 38), these transformations proceeded *via* a stepwise pathway, commencing with nucleophilic attack of the indole's C_2/C_3 position on the terminal allene carbon to generate dearomatized cationic intermediates **174/175**. The regioselectivity on the allene substrates was governed by the electron-withdrawing group on the nitrogen. The second bond was formed by intramolecular cyclization on the C–Au bond, thus affording the final products and regenerating the Au(I) catalyst.

In 2017, the Mikami group realized the first gold(I)-catalyzed asymmetric intermolecular [4+2] cycloadditions between 1,3-dienes and ynones.[124] Using pyrrolidyl phosphoramidite **L28** as the chiral ligand, bicyclo[2.2.2]octadiene derivatives **178** were obtained in high yields and enantioselectivities from cyclohexadiene **176** and ynones **177** (Scheme 39). In control experiments, when substituted ynones were utilized as substrates, the desired

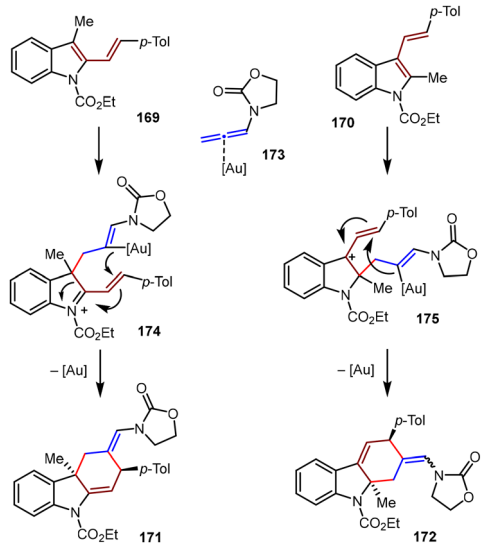

Scheme 38 Proposed mechanism for the Au(I)-catalyzed [4+2] cycloadditions of substituted vinylindoles and *N*-allenamides.

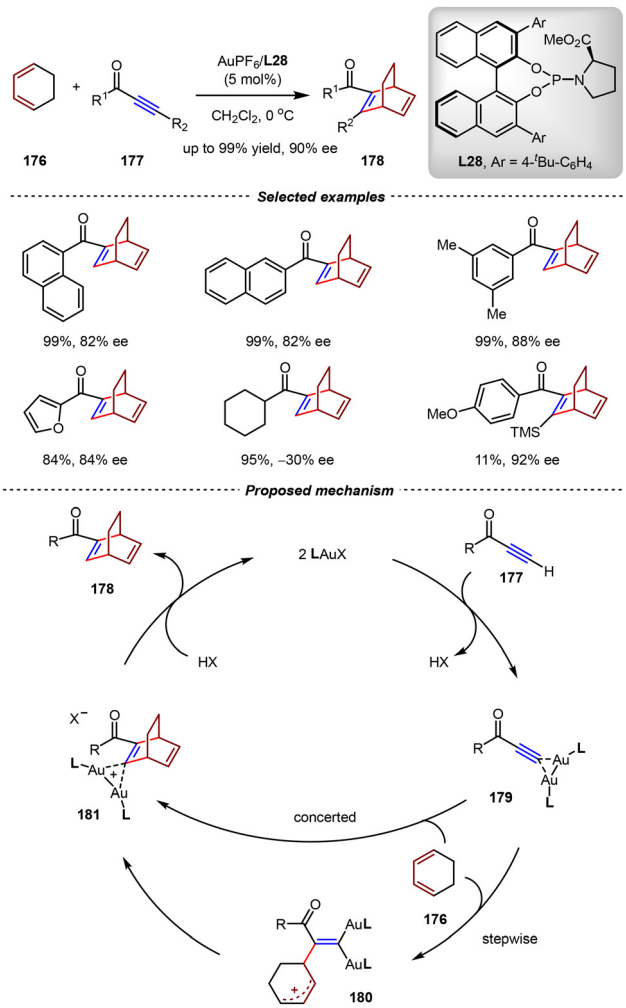

Scheme 39 Au(I)/phosphoramidite-catalyzed asymmetric intermolecular [4+2] cycloadditions of ynones and cyclohexa-1,3-dienes.

Open Access Article. Published on 13 2026. Downloaded on 08/05/26 22:54:22.
This article is licensed under a Creative Commons Attribution 3.0 Unported Licence.

products could not be afforded or generated in very low yields, thus indicating the key role of terminal alkynes in this transformation. Systematic investigations, including NMR studies and non-linear effect experiments, suggested the existence of the *gem*-digold ynone complex. In a proposed catalytic cycle, *gem*-digold species **179** was initially generated. Then, the Diels–Alder reaction of **179** with the cyclohexadiene occurred efficiently in a stepwise or concerted reaction pathway.

The resulting *gem*-digold intermediate **181** was protonated to release the chiral bicyclo[2.2.2]octadiene product and regenerate the cationic Au(I) catalyst.

4. Enantioselective [4+2] cycloadditions *via* the HOMO activation of π-bases

In contrast to electrophilic Au(I) complexes, which demonstrated a weak π-backdonation ability, some low-valent metals exhibited stronger π-backdonation than σ-donation when complexed with alkenes or alkynes, thus serving as π-Lewis bases to increase the electron density of unsaturated hydrocarbons. Based on this mode, Harman and others developed various impressive transformations of inert arenes and 1,3-dienes by the π-base activation of Os(II), Rh(I), Mo(0), and W(0) complexation.[125–131] Very recently, a breakthrough in this research field was made by the Chen group, who identified that Pd(0) complexes could serve as π-Lewis base catalysts.[51,132–136] By increasing the HOMO energy of unsaturated hydrocarbons, many types of reactions, including some unprecedented [4+2] cycloadditions, were realized elegantly.

Cyclopentadienones were privileged electron-deficient dienes in Diels–Alder reactions, which were widely used in the synthesis of polycyclic aromatic hydrocarbons (PAHs).[137–139] However, the parent cyclopentadienone without substituents was rarely utilized in organic synthesis owing to its high tendency to undergo self-dimerization.[140–142] In 2021, the Chen group disclosed that 4-hydroxy-2-cyclopentadienone carbonates could be used as precursors of cyclopentadienones (Scheme 40).[143] In the presence of a Pd(0) catalyst, the oxidative addition of the 4-hydroxy-2-cyclopentenone carbonate produced the key π-allylpalladium intermediate **183**, which then underwent α-deprotonation and isomerization (β-H elimination) to afford the cyclopentadienone intermediate. By forming η^2-complex **185** with the regenerated Pd(0) catalyst, the cyclopentadienone was stabilized, thus avoiding the facile dimerization. Remarkably, the HOMO energy of **185** was raised to −5.26 eV (*vs.* −7.03 eV for free cyclopentadienone) by the π-backbonding from the Pd(0) center as the π-Lewis base, thus enabling the uncoordinated alkene in cyclopentadienone as an electron-rich dienophile in inverse-electron-demand Diels–Alder (IEDDA) reactions.

Using the $Pd_2(dba)_3$/**L29** complex as the π-Lewis base catalyst, the umpolung aza-type IEDDA reactions between 4-hydroxy-2-cyclo-pentenone derivatives **187** and 1-azadienes **188** were realized. Notably, these reactions demonstrated excellent functional group tolerance toward 1-azadienes **188**, affording chiral nitrogen atom-fused cyclic products **189** in high yields and outstanding enantioselectivities (up to 98% yield, 99% ee, >19 : 1 dr, Scheme 40). Additionally, employing

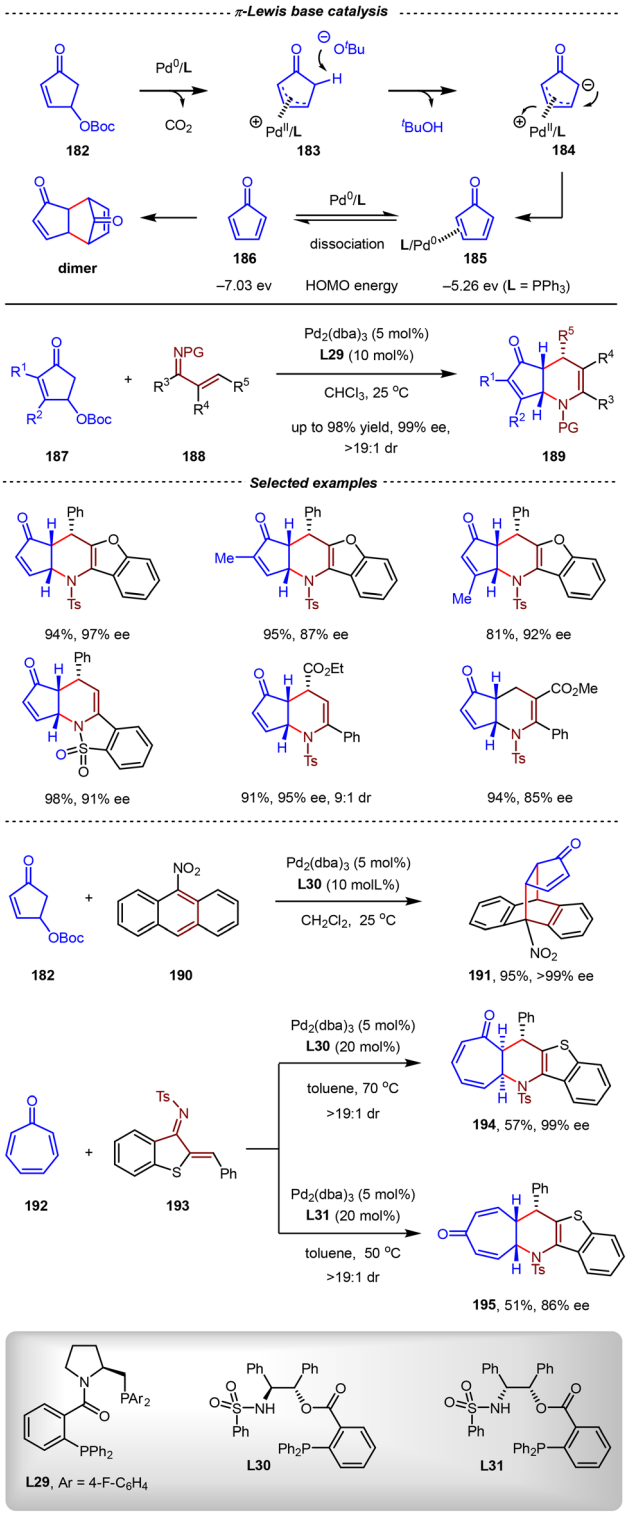

Scheme 40 Pd(0)-catalyzed umpolung asymmetric inverse-electron-demand Diels–Alder reactions of 4-hydroxy-2-cyclopentenone carbonates.

This journal is © The Royal Society of Chemistry 2026

Open Access Article. Published on 13 2026. Downloaded on 08/05/26 22:54:22.
This article is licensed under a Creative Commons Attribution 3.0 Unported Licence.

L30 as the chiral ligand, 9-nitroanthracene **190** could also be used effectively as a diene partner, yielding the bridged [4+2] cycloadduct **191** with 95% yield and >99% ee. Intriguingly, cycloheptatrienone **192** was also an effective electron-rich 2π component in aza-Diels–Alder cyclization with 1-azadiene **193**. Notably, the regioselectivity was controlled by ligands. Regiodivergent cycloadducts **194** and **195** were afforded in moderate yields and high enantioselectivities by the utilization of **L30** and **L31**, respectively.

Based on the same π-Lewis base activation strategy, the Chen group developed the Pd(0)-catalyzed asymmetric inverse-electron-demand oxa-Diels–Alder reactions between 4-hydroxy-2-cyclopentenone carbonates **187** and α,β-unsaturated ketones **196** (Scheme 41).[144] By this method, a series of chiral fused dihydropyrans **197** with versatile structural and functional diversity, generally with high stereoselectivity, could be constructed by the utilization of bifunctional aminoalcohol-derived monophosphine ligand **L30** or proline-derived bisphosphine ligand **L32**. Remarkably, a ligand-dependent stereodivergence was observed. Employing **L30** as the chiral ligand produced *exo*-cycloadducts exclusively (up to >19:1 dr), while the utilization of **L32** furnished *endo*-cycloadducts with high diastereoselectivities (up to >19:1 dr). DFT calculations revealed that the [4+2] cycloaddition exhibited a concerted reaction pathway between the *in situ* generated η^2-Pd(0)-cyclopentadienone complex and α,β-unsaturated ketone. With **L30** as the ligand, a hydrogen-bonding interaction was observed between the N–H group of the ligand and the O-atom of cyclopentadienone in the [4+2] cycloaddition transition state, thus forcing the cycloaddition to proceed in an *exo*-fashion.

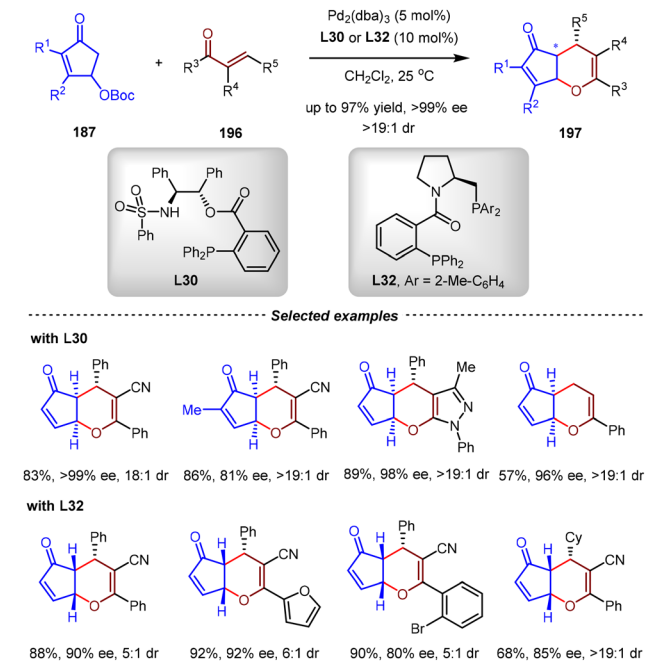

Scheme 41 Pd(0)-catalyzed umpolung asymmetric inverse-electron-demand oxa-Diels–Alder reactions of 4-hydroxy-2-cyclopentenone carbonates and α-cyano chalcones.

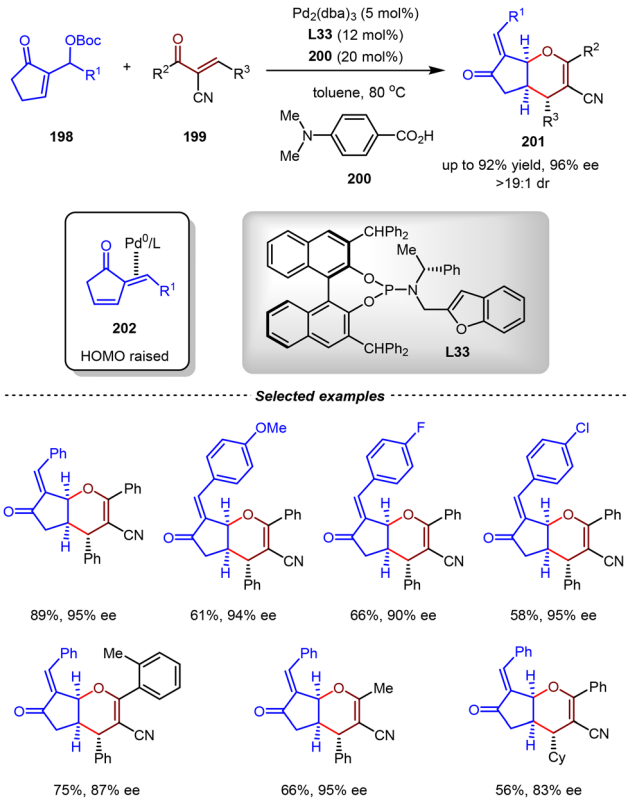

Scheme 42 Pd(0)-catalyzed asymmetric inverse-electron-demand oxa-Diels–Alder reactions of MBH carbonates and α-cyano chalcones.

To expand the generality of the Pd(0)-catalyzed asymmetric IEDDA reactions, the Chen group disclosed that dienones generated from Morita–Baylis–Hillman (MBH) carbonates **198** could be umpolunged to serve as electron-rich dienophile components (Scheme 42).[145] By regioselective coordination of the Pd(0) catalyst on the *exo*-double bond, η^2-Pd(0)-dienone complexes **202** were formed, with raised HOMO energy of the *endo*-double bond through π-Lewis base activation. By the utilization of $Pd_2(dba)_3$/**L33** and **200** as co-catalysts, enantioselective inverse-electron-demand oxa-Diels–Alder reactions between MBH carbonates **198** and α-cyano chalcones **199** were realized. Based on this method, a variety of *cis*-pyran derivatives **201** with fused architectures were produced efficiently with high yields, high enantioselectivities, and high diastereoselectivities (up to 92% yields, 96% ee, >19:1 dr).

In 2023, the same group reported asymmetric 2,4-dienylation/intramolecular [4+2] cycloaddition cascade reactions by tandem Pd(0) catalysis (Scheme 43).[146] The reaction commenced with the intermolecular allylation between *ortho*-functionalized aryl enones **203** and 2,4-dienyl carbonates **204** to give the dienyl enone intermediate **206**. Then, the HOMO energy of the diene moiety of **207** was raised by π-Lewis base activation of the Pd(0) catalyst, thus facilitating the enantioselective intramolecular 1,4-addition. After the π–σ–π allylic isomerization, the resulting η^3-complex underwent the intramolecular allylic alkylation to produce the final product. Using **L34** as the chiral ligand, various *ortho*-functionalized aryl

Open Access Article. Published on 13 2026. Downloaded on 08/05/26 22:54:22.
This article is licensed under a Creative Commons Attribution 3.0 Unported Licence.

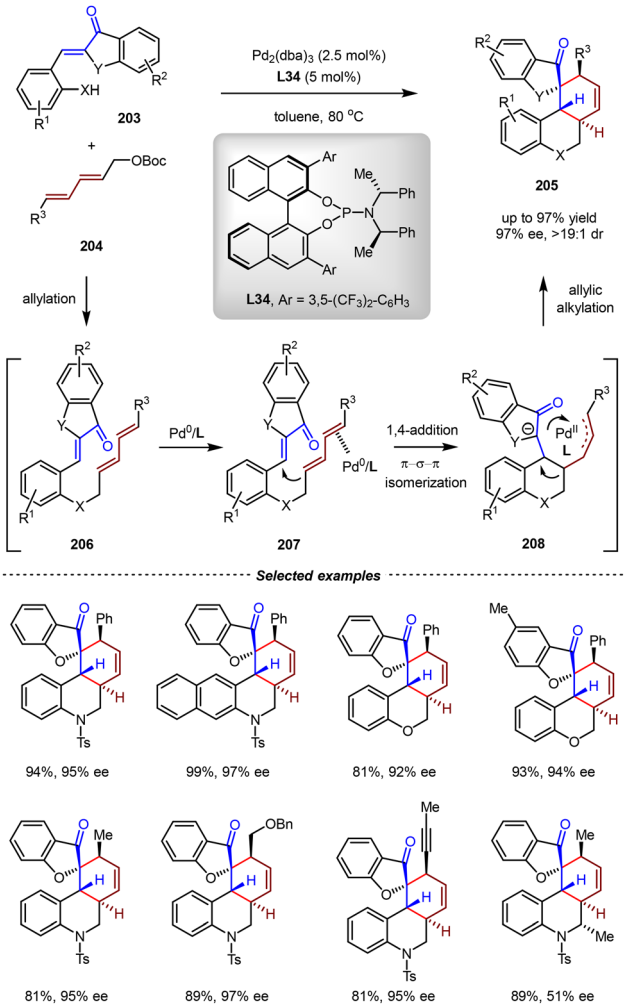

Scheme 43 Pd(0)-catalyzed tandem asymmetric Tsuji–Trost allylation and intramolecular [4+2] cycloaddition reactions.

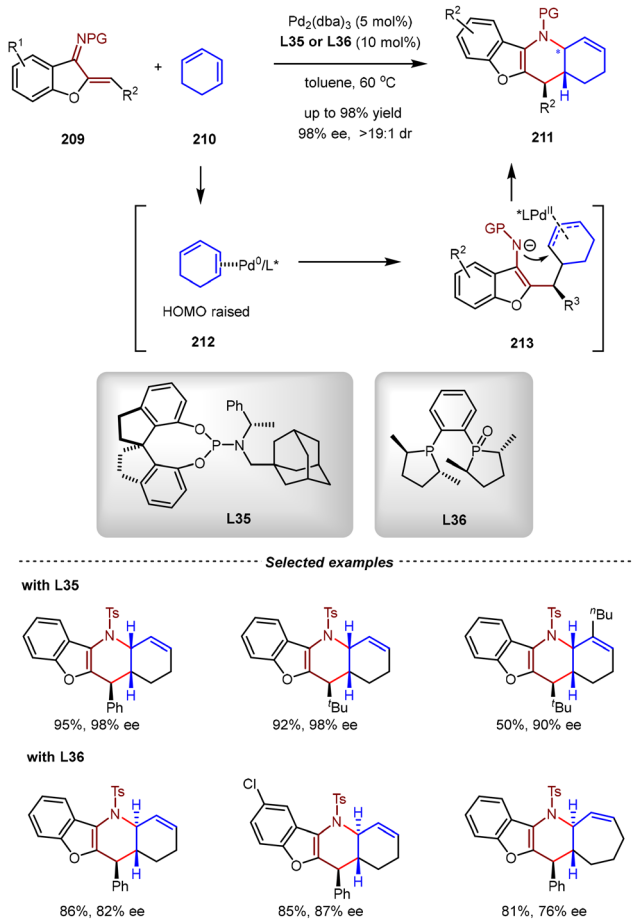

Scheme 44 Pd(0)-catalyzed formal inverse-electron-demand aza-Diels–Alder reactions between 1,3-cyclohexadiene and aurone-derived 1-azadienes.

enones and 2,4-dienyl carbonates bearing aryl, alkyl, and alkynyl substituents were compatible in this cascade reaction, affording a wide range of enantioenriched spirocyclic architectures **205** with good yields and excellent ee (up to 97% yield, 97% ee).

It has been reported that in uncatalyzed IEDDA reactions of aurone-derived 1-azadienes **209** and 1,3-cyclohexadiene **210**, the *endo*-selectivity was often observed, giving *cis*-fused polycyclic product exclusively. In 2023, the Chen group demonstrated that the diastereoselectivity of this reaction could precisely be reversed by the ligand. In the presence of catalytic amounts of $Pd_2(dba)_3$ and **L35**, [4+2] cycloadditions of **209** and **210** proceeded in an *exo* fashion, giving *cis*-fused tetrahydropyridine cycloadduct **211** in high yields and enantioselectivities (up to 99% yield, 98% ee) (Scheme 44).[147] It was proposed that the coordination of the Pd(0) catalyst with **210** generated HOMO-energy-elevated η^2-Pd(0) complex **212**, which then underwent 1,4-addition with **209**. From the resulting allylic Pd(II) species, the subsequent intramolecular allylic amination afforded the final product and regenerated the Pd(0) catalyst. By judicious selection of chiral ligand **L36**, the diastereoselectivity of the [4+2] annulation was switched, leading to the construction of *trans*-fused tetrahydropyridines **211** as main products (up to 98% yield, 98% ee, >19 : 1 dr). Remarkably, 1,3-cyclopentadiene, 1,3-cycloheptadiene, and acyclic 1,3-dienes were also compatible in the reaction, thus highly expanding the reaction generality.

In 2024, the Chen group reported a relay catalytic strategy involving Au-catalyzed cycloisomerization and Pd(0)/CPA co-catalyzed asymmetric [4+2] cycloaddition between enynamides **214** and 4-hydroxy-2-cyclopentenone carbonate derivatives **182** (Scheme 45).[148] The reaction sequence commenced with the $Ph_3PAuNTf_2$-catalyzed intramolecular 5-*endo-dig* cyclization of enynamides **214**, which efficiently generated dihydrofuran-fused azadiene intermediates **216**. Subsequently, a cooperative catalytic system comprising $Pd_2(dba)_3$/**L37** and chiral phosphoric acid **217** enabled the asymmetric formal [4+2] cycloadditions between *in situ* formed dihydrofuran-fused azadiene intermediates **216** and 4-hydroxyl-2-cyclopentanone carbonates **182**. In line with previous studies (Scheme 40), carbonates **182** were proposed to convert to the corresponding η^2-Pd(0)-cyclopentadienone intermediates *via* sequential oxidative addition,

This journal is © The Royal Society of Chemistry 2026

Open Access Article. Published on 13 2026. Downloaded on 08/05/26 22:54:22.
This article is licensed under a Creative Commons Attribution 3.0 Unported Licence.

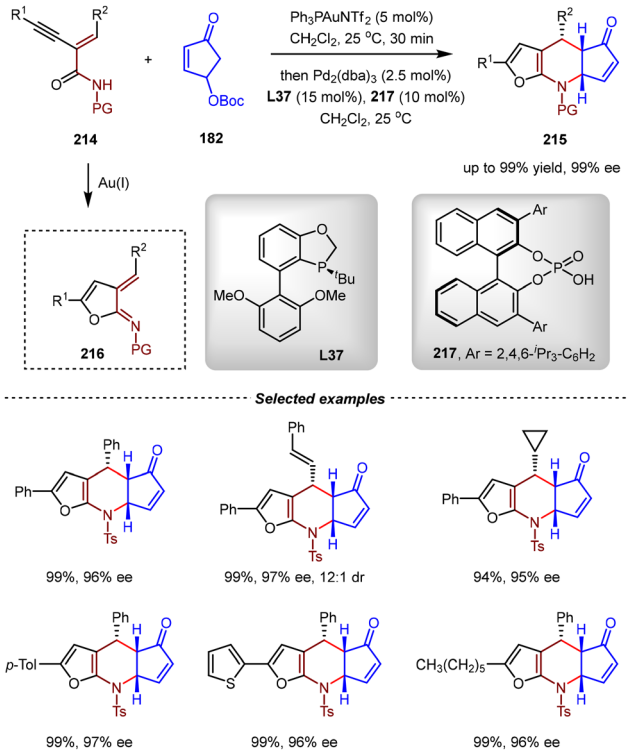

Scheme 45 Asymmetric synthesis of furo[2,3-b]pyridines by sequential Au(I) and Pd(0)/chiral phosphoric acid catalysis.

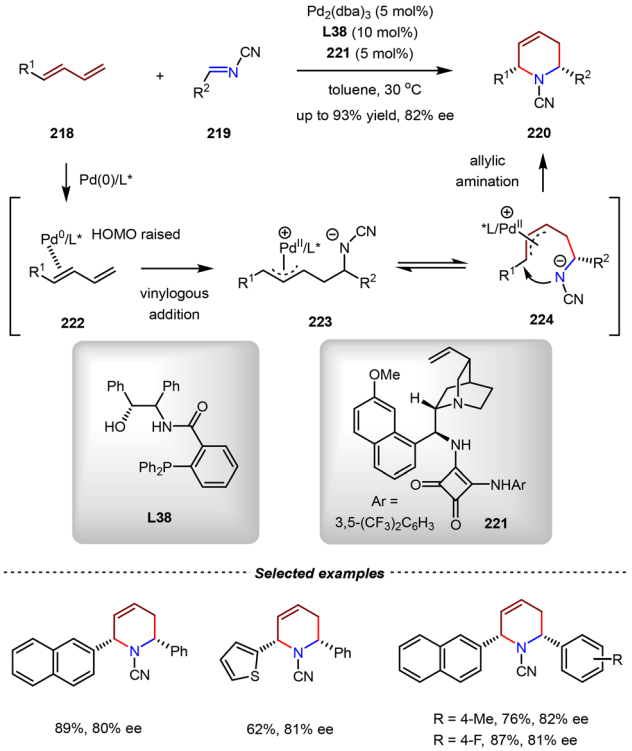

Scheme 46 Pd(0)-catalyzed asymmetric aza-[4+2] cycloadditions of acyclic 1,3-dienes with *N*-cyano imines.

α-deprotonation and isomerization. Owing to the strong back-bonding effect of the Pd(0) catalyst, the cyclopentadienone could serve as an electron-rich dienophile to react with **216**. Remarkably, this cascade process demonstrated a wide reaction scope, affording various 6,7-dihydro-5*H*-cyclopenta[*b*]furo[3,2-*e*] pyridine scaffolds with excellent yields and enantioselectivities (up to 99% yield, 99% ee).

An enantioselective formal aza-[4+2] cycloaddition between 1,3-dienes and *N*-cyano imines was realized by Pd(0)–π-Lewis base catalysis (Scheme 46).[149] By the combination of $Pd_2(dba)_3$, monophosphine ligand **L38**, and chiral squaramide **221**, the [4+2] cycloadditions of **218** and **219** went on smoothly to afford multifunctional piperidine derivatives with high yields and moderate enantioselectivities (up to 93% yield, 82% ee). In a proposed mechanism, 1,3-dienes **218** were activated by the Pd(0) catalysis with elevated HOMO energy, thereby promoting the vinylogous 1,2-addition with electron-deficient *N*-cyano imines **219**. The resulting allylic Pd(II) intermediate **223** underwent the subsequent intramolecular allylic amination to give the final product and regenerate the Pd(0) catalyst. It should be noted that the enantioselectivity was controlled by chiral squaramide **221**, which served as a Brønsted acid to increase the electrophilicity of **219**.

The cross-Diels–Alder reaction between two different 1,3-dienes often gave a complex mixture, owing to the challenge in controlling the periselectivity, regioselectivity, and stereoselectivity simultaneously. As we mentioned before, Cramer and Braconi realized the enantioselective cross-[4+2] cycloaddition between two different unactivated 1,3-dienes by iron catalysis (Scheme 29).[102] In 2024, the Cai group reported a cooperative Pd(0)/chiral phosphoric acid catalytic system, enabling the first chemo-, regio- and enantioselective sequential cross-[4+2] cycloaddition/decarboxylation of 2-pyrones[150–152] **225** with unactivated acyclic 1,3-dienes **226** (Scheme 47).[153] By this method, a wide range of chiral vinyl-1,3-cyclohexadiene derivatives **227**, which were challenging to be accessed by other methods, were obtained under mild reaction conditions with excellent yields and enantioselectivities (up to 92% yield, 99% ee).

Based on systematic experimental investigations and DFT calculations, a reasonable mechanism was proposed (Scheme 47). The catalytic cycle of the [4+2] cycloaddition was initiated with the coordination of 1,3-diene **226** with the Pd(0)/**L39** complex, forming the η^2-complex **229** with increased nucleophilicity by π-backbonding from the Pd(0) center interaction. Concurrently, the electrophilicity of 2-pyrone **225** was elevated by hydrogen-bonding activation with the sterically hindered chiral phosphoric acid **228**. This synergistic catalytic system enabled the stereoselective 1,6-addition of complex **229** to 2-pyrone **225**, generating the zwitterionic intermediate **231**. Regioselective intramolecular palladium-catalyzed allylic substitution then occurred at the C3 position of **225**, giving the *exo*-cycloadduct **232** as the key intermediate. In the decarboxylation cycle, the lactone group of **233** was activated by **228**, thus promoting the oxidative addition with the Pd(0)/**L39** complex from the back of the lactone moiety. Since the palladium center was far away from the nascent carboxylic group in the resulting intermediate

Open Access Article. Published on 13 2026. Downloaded on 08/05/26 22:54:22.
This article is licensed under a Creative Commons Attribution 3.0 Unported Licence.

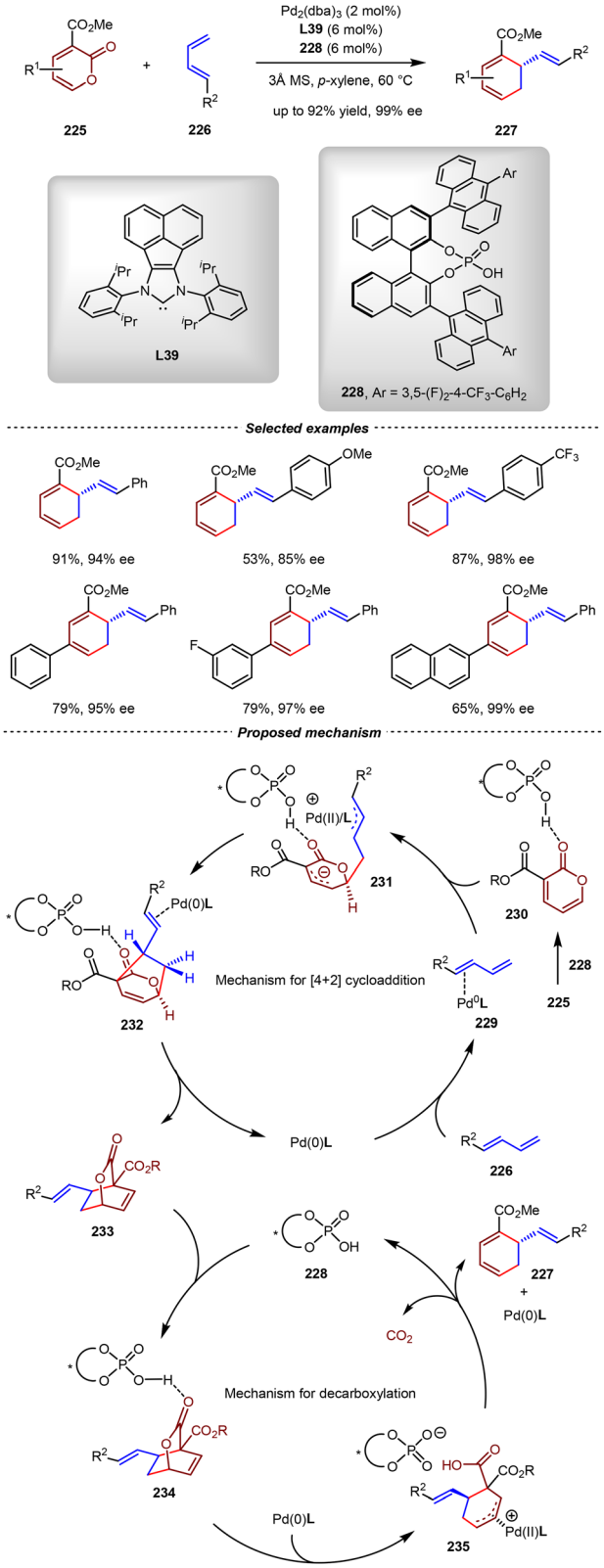

Scheme 47 Pd(0)/chiral phosphoric acid co-catalyzed periselective and enantioselective cross-[4+2] cycloaddition and decarboxylation reactions.

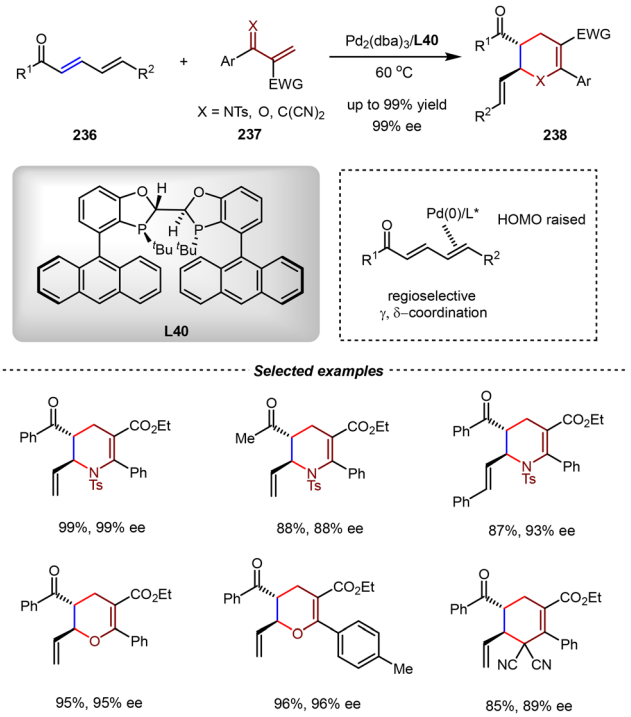

Scheme 48 Pd(0)-catalyzed asymmetric cross inverse-electron-demand [4+2] cycloadditions between 2,4-dienyl carbonyls and 1-heterodienes/allylidenemalononitriles.

235, the decarboxylation occurred directly without the assistance of Pd(II). This step furnished the final 1,3-cyclohexadiene product **227** while regenerated both the Pd(0) catalyst and chiral phosphoric acid **228** to complete the catalytic cycle. Notably, the key for the success of this transformation was the utilization of an achiral NHC ligand, which highly increased the electron density of the palladium center.

In 2024, the Chen group reported the regioselective and enantioselective cross inverse-electron-demand [4+2] cycloadditions between 2,4-dienyl carbonyls and 1-heterodienes or allylodenemalononitriles by the Pd(0)–π-Lewis base catalysis (Scheme 48).[154] In these reactions, the reactivity of the electron-deficient dienes **236** was reversed by regioselective γ,δ-η^2 coordination with the Pd(0) catalyst, which donated its d-electron by π-backbonding, thus rendering **236** as electron-rich dienophiles in [4+2] cycloadditions with **237**. By the combination of catalytic amounts of $Pd_2(dba)_3$ and the chiral ligand **L40**, various types of 1-heterodienes or allylodenemalononitriles were compatible in this reaction, affording a wide range of multifunctional six-membered cyclic compounds **238** with excellent yields and enantioselectivities (up to 99% yield and 99% ee).

5. Catalytic asymmetric radical-mediated [4+2] cycloadditions

Free radical reactions play a central role in organic synthesis owing to their high reactivity and efficiency.[155–160] In recent years, radical-mediated [4+2] cycloadditions have received widespread interest from the synthetic community.[161,162] Compared

This journal is © The Royal Society of Chemistry 2026

Open Access Article. Published on 13 2026. Downloaded on 08/05/26 22:54:22.
This article is licensed under a Creative Commons Attribution 3.0 Unported Licence.

with the classic ionic Diels–Alder reaction, which typically occurs between an electron-rich component and an electron-deficient partner, the radical-mediated [4+2] cycloaddition could utilize simple and electronically mismatched unsaturated hydrocarbon substrates, thus making this reaction more general.[51–56] However, due to the lack of catalytic modes to manipulate the stereochemistry of highly reactive radical species, the development of catalytic asymmetric radical-mediated [4+2] cycloaddition remains a challenging topic in organic synthesis. It is not until very recently, a few breakthroughs have emerged, which are deemed to be inspiring for more research work in this field. In this section, we will discuss these advancements according to the mechanistic reaction pathways.

5.1. Catalytic asymmetric radical cation [4+2] cycloadditions

Electronically mismatched Diels–Alder reactions between two electron-rich components are regarded as one of the most challenging reaction modes, which often require harsh reaction conditions and a longer reaction time. In this regard, the radical cation Diels–Alder reaction is highly attractive. In the presence of an oxidative electron transfer catalyst, the reaction proceeds through one-electron oxidation of the electron-rich olefins to form a radical cation intermediate, followed by the subsequent cycloaddition with electron-rich dienes, thereby increasing the reaction rate by several orders of magnitude. Since the pioneering work of Bauld and co-workers, the radical cation Diels–Alder reaction has been extensively investigated by the development of one-electron oxidative catalysts, such as ground-state aminium salts, Fe(III) salts, and photoinitiated electron transfer with organic photosensitizers.[163–171] Despite these great achievements, catalytic asymmetric radical cation [4+2] cycloadditions remain elusive, and only two examples have been reported to date.

The first catalytic asymmetric radical cation [4+2] cycloaddition was reported by the Nicewicz group in 2018 (Scheme 49).[172] By the development of a novel class of photoredox catalytic system comprising an oxidizing triaryl pyrylium (TP) salt bearing a chiral *N*-triflyl phosphoramide counterion, the intramolecular [4+2] cycloadditions of unactivated diene-enes **239** were achieved successfully, albeit with moderate enantioselectivities (up to 50% ee). In a proposed mechanism, the reaction was initiated by single-electron oxidation of the olefin moiety in diene-ene **239** *via* the excited-state catalyst **241**, thus generating radical cation intermediate **242**. Subsequent intramolecular cycloaddition of **220** gave radical cation intermediate **243**, which then underwent single-electron reduction to furnish the final *trans*-5,6-fused bicycle products **240**, while simultaneously regenerating the catalyst. Although only moderate enantioselectivities were obtained for the desired products, this study made an important proof-of-concept that ion pairing between radical cation intermediates and chiral anions was capable of inducing enantiocontrol in radical cation [4+2] cycloadditions.

A breakthrough in this research field was made by the Ishihara group very recently (Scheme 50).[173] In 2023, they reported a judicious design of a chiral Fe(III) photoredox

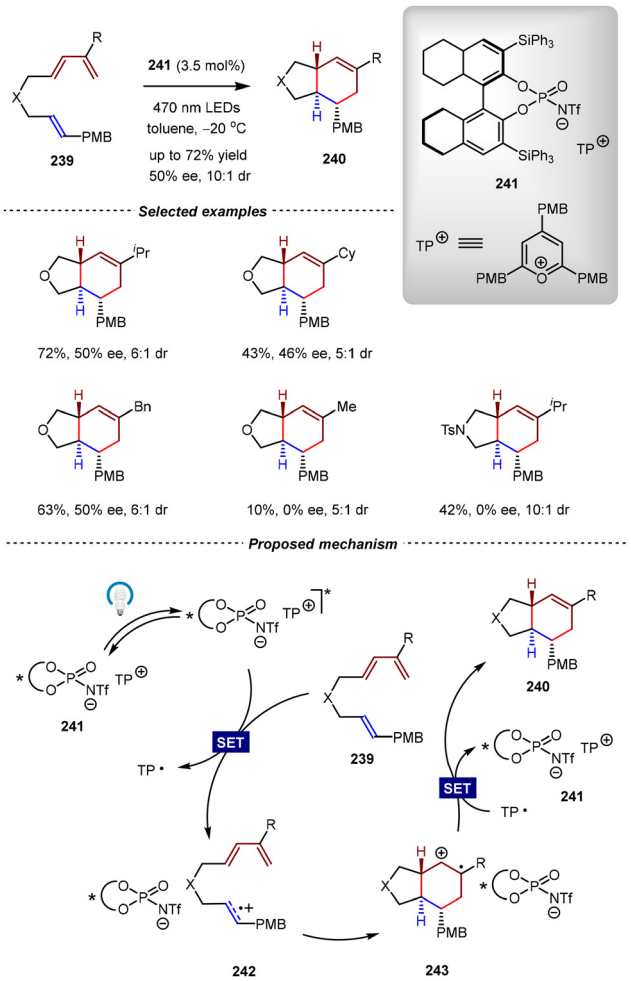

Scheme 49 Cationic oxopyrylium-catalyzed asymmetric radical cation intramolecular [4+2] cycloadditions of unactivated diene-enes.

catalyst generated *in situ* from $FeCl_3$ and a chiral silver(I) phosphate salt. In the presence of catalytic amounts of $FeCl_3$ (5 mol%) and silver phosphoramide **247** (16.5 mol%), the intermolecular [4+2] cycloadditions between chalcone derivatives **245** and isoprene **244** went on smoothly to provide the corresponding cycloadducts **246** in good yields with high enantioselectivities (up to 81% yield, 94% ee). It should be noted that the methyl group of **246** was at the *meta*-position of the carbonyl group, which exhibited the opposite regioselectivity compared with Lewis acid-mediated Diels–Alder reactions based on the Woodward–Hoffmann rule.

In a proposed mechanism, $FeCl_3$ underwent anion exchange with three equivalents of **247** to generate the chiral FeX_3 salt *in situ*. Upon irradiation with blue LEDs, this Fe(III) complex was excited and subsequently quenched with the chalcone derivative **245** through one-electron oxidation to afford FeX_2 and radical cation intermediate **248** paired with the chiral phosphoramide anion (X^-). The stereochemistry of the subsequent radical cation-induced [4+2] cycloaddition of **248** was controlled by the chiral anion to produce the radical cation intermediate **249**. Finally, the one-electron reduction of **250**

Open Access Article. Published on 13 2026. Downloaded on 08/05/26 22:54:22.
This article is licensed under a Creative Commons Attribution 3.0 Unported Licence.

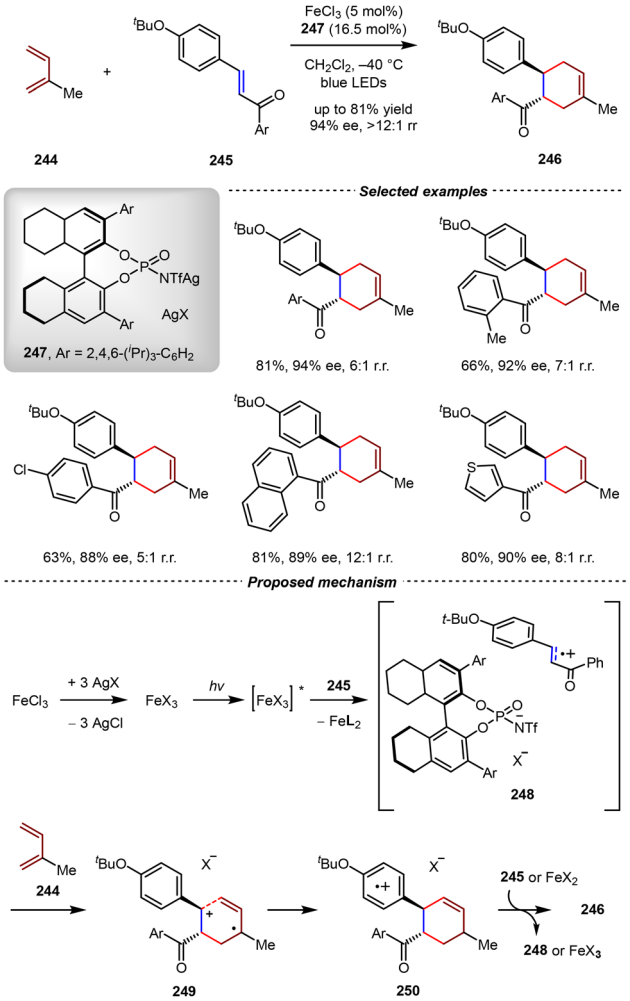

Scheme 50 Asymmetric radical cation [4+2] cycloadditions catalyzed by the combination of $FeCl_3$ and silver *N*-triflylphosphoramide.

with FeX_2 or chalcone derivative **245** delivered the cyclohexene product **246** with good enantioselectivities. Notably, this catalytic system was also applicable to the intermolecular asymmetric [2+2] cycloadditions of chalcone derivatives and styrenes, thus demonstrating the generality of this chiral counteranion strategy.

According to the above proposed mechanism, only one chiral phosphoramide anion (X^-) was involved in the enantiodetermining step. Consequently, the Ishihara group then developed a new chiral Fe(III) photoredox catalyst, which consisted of a chiral phosphoramide anion and an achiral bidentate ligand (Scheme 51).[174] By the catalysis of the *in situ* generated **253** from $FeCl_3$, achiral disilver salt **254**, and silver phosphoramide **247**, the intermolecular [4+2] cycloadditions between chalcone derivatives **251** and 1,3-butadiene derivatives **252** proceeded enantioselectively, leading to the corresponding cycloadducts with high yields and ee. By this strategy, only one equivalent of the chiral silver salt was needed. Notably, this new catalysis design also benefitted from the tunability of the achiral ligand in the disilver salt to achieve good stereocontrol.

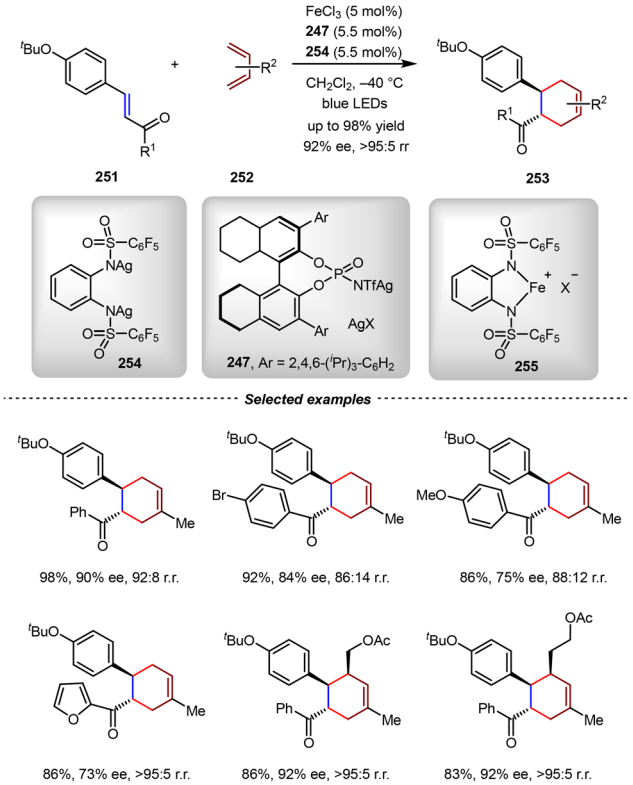

Scheme 51 A new Fe(III) photocatalyst consisting of a chiral phosphoramide anion and an achiral bidentate ligand.

5.2. Catalytic asymmetric triplet-state [4+2] cycloadditions

Besides the single-electron-transfer (SET) reaction pathway, the photocatalysis through the energy transfer process has also emerged as a powerful approach to facilitate [4+2] cycloadditions that are hard to be achieved by traditional methods.[53] However, the high reactivity of radical species and excited-state intermediates poses an impetus to achieving high enantiocontrol by chiral catalysts. In 1990, the Schuster group reported the first enantioselective photochemical [4+2] cycloaddition.[175] By the catalysis of enantioenriched (–)-1,1′-bis(2,4-dicyanonaphthalene) [BDCN] **259** (2.5 mol%, 70% ee) under irradiation (350 nm) in toluene, the [4+2] cycloaddition between 1,3-cyclohexadiene (CHD) **256** and *trans*-β-methylstyrene **257** gave the corresponding cycloadduct **258** in 15% ee (Scheme 52). Mechanistically, it was proposed that photosensitizer **259** initially formed a pair of diastereomeric exciplexes with prochiral

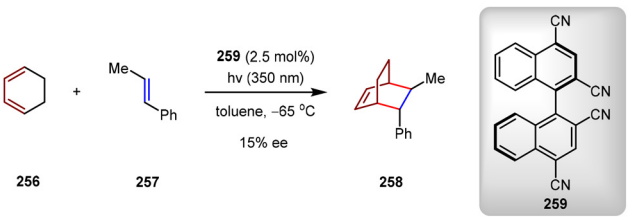

Scheme 52 The BDCN-catalyzed photosensitized [4+2] cycloaddition of *trans*-β-methylstyrene with 1,3-cyclohexadiene.

This journal is © The Royal Society of Chemistry 2026

Open Access Article. Published on 13 2026. Downloaded on 08/05/26 22:54:22.
This article is licensed under a Creative Commons Attribution 3.0 Unported Licence.

dienophile **257** by different facial orientations, which then reacted with CHD **256** to form a triplex, thereby enabling the subsequent [4+2] cycloaddition. The observed enantioselectivity originated from the selective capture of the diastereomeric exciplexes with CHD **256**, establishing the stereochemical basis for the asymmetric induction in this transformation.

The first catalytic asymmetric photochemical [4+2] cycloadditions with high enantiocontrol were reported by the Jiang group in 2024 (Scheme 53).[176] By the cooperative catalysis of photosensitizer dicyanopyrazine (DPZ) **263** and chiral phosphoric acid **264**, the dearomative [4+2] cycloadditions between anthracenes **260** and alkenyl-azaarenes **256** went on smoothly under irradiation of visible light. By this method, a series of high-value cycloadducts incorporating the privileged azaarene motif were obtained in excellent yields with high enantioselectivities and diastereoselectivities (up to 99% yield, 99% ee, and >20 : 1 dr). The synthetic utility was unambiguously demonstrated by the construction of all-carbon quaternary stereocenters bearing multiple adjacent stereocenters. In a plausible mechanism, the DPZ sensitizer underwent intersystem crossing (ISC) to generate the triplet excited state ^{3}DPZ. Subsequent triplet–triplet energy transfer of ^{3}DPZ with **255** gave the triplet diradical species **260**. Meanwhile, alkenyl-azaarene **261** complexed with chiral Brønsted acid **264** *via* the hydrogen-bonding interaction to establish a chiral environment for the subsequent radical addition with **266**. The resulting diradical intermediate **267** underwent ISC followed by the diradical coupling, affording final [4+2] cycloadduct **262**. It should be noted that the pyrene groups on the chiral phosphoric acid were essential

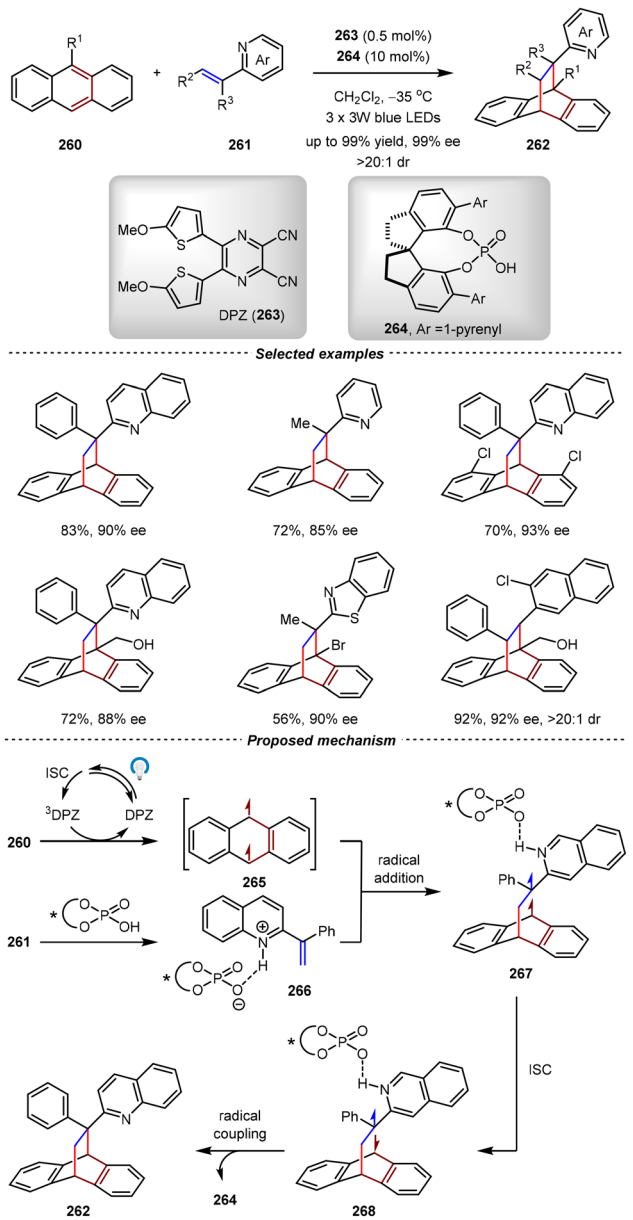

Scheme 53 Asymmetric [4+2] dearomative photocycloadditions of anthracene with alkenylazaarenes.

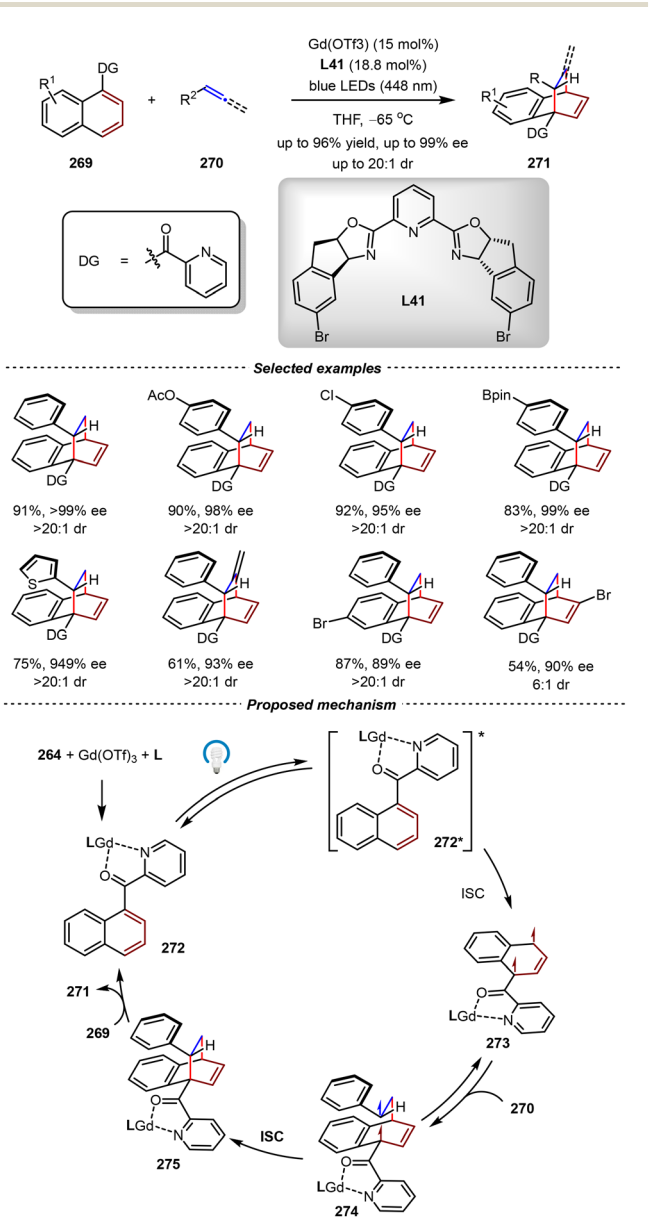

Scheme 54 Gd(III)-catalyzed asymmetric [4+2] photocycloadditions of naphthalenes and styrenes.

Open Access Article. Published on 13 2026. Downloaded on 08/05/26 22:54:22.
This article is licensed under a Creative Commons Attribution 3.0 Unported Licence.

for the good enantioselectivity control, which were proposed to have π–π stacking interactions with substrates.

Almost at the same time, the You group reported the Lewis acid catalyzed asymmetric dearomative (CADA) [4+2] cycloadditions of naphthalene derivatives (Scheme 54).[177] By the catalysis of $Gd(OTf)_3$ and PyBox **L41** under visible light irradiation, the dearomative [4+2] cycloadditions of naphthalenes and styrenes delivered a diverse range of bridged polycyclic products with excellent yields and enantioselectivities (up to 96% yield, >99% ee, >20:1 dr, and >20:1 rr). Notably, phenyl allene also showed good reactivity, giving the corresponding diene product in 61% yield and 93% ee. By extensive mechanistic investigations, it was found that the Gd(III)/**L41** complex served dually as both the excited-state catalyst and the stereocontrol modulator. Initially, the coordination of Gd(III)/**L41** with **269** produced ground-state intermediate **272**, which then generated singlet excited-state **272*** under blue LED irradiation. From **272***, triplet-state intermediate **273** was afforded *via* ISC. This reactive diradical species then mediated the stereoselective *Si*-face addition with **270**, producing a new biradical intermediate **274**. The subsequent ISC process enabled the intramolecular radical recombination to give intermediate **275**, which then underwent ligand exchange with **269**, thus simultaneously releasing the desired product **271** and regenerating intermediate **272** to complete the catalytic cycle. This effective photocatalytic dearomatization strategy opened a new gate for the development of future photochemical asymmetric [4+2] cycloaddition reactions.

6. Conclusions

Over the past three decades, the field of organic synthesis has witnessed remarkable progress in catalytic asymmetric [4+2] cycloadditions involving alkenes, alkynes, and allenes, extending well beyond the conventional Diels–Alder reaction. Transition metal catalysis, in particular, enables these transformations by coordinating with unsaturated C–C bonds in reactants and facilitating subsequent oxidative cyclometallation and reductive elimination to afford [4+2] cycloadducts. Through careful selection of transition metals and ligands, high levels of chemo-, regio-, and stereoselectivity of [4+2] cycloadditions can be achieved. On another front, π-acidic Au(I) catalysts activate allenes to generate highly reactive Au-allyl cation species, which readily undergo intramolecular or intermolecular [4+2] cycloadditions with 1,3-dienes. More recently, low-valent Pd(0) complexes have emerged as efficient π-Lewis base catalysts that raise the HOMO energy of unsaturated hydrocarbons *via* η^2 coordination, enabling previously inaccessible [4+2] cycloadditions. Notably, photo-induced catalytic asymmetric [4+2] cycloadditions proceeding *via* the radical cation or triplet-state pathway have introduced unique and powerful reaction modes. By these innovative strategies, [4+2] cycloadditions have been significantly extended to unactivated unsaturated hydrocarbons, which are typically unreactive substrates under conventional Diels–Alder reactions.

Despite the notable achievements realized to date, the reaction scope and patterns of [4+2] cycloadditions beyond conventional Diels–Alder reactions remain limited. In transition metal-catalyzed [4+2] cycloadditions following the oxidative cyclometallation/reductive elimination pathway, current studies are predominantly focused on intramolecular reactions. In contrast, intermolecular [4+2] cycloadditions are rare and often suffer from low reactivity, along with poor control over stereoselectivity and regioselectivity. Regarding π-acid and π-base activation modes, only Au(I) and Pd(0) complexes have been employed as catalysts, leaving other transition metals largely unexplored. Notably, catalytic asymmetric radical-mediated [4+2] cycloadditions are still in infancy, especially when compared to the rapidly advancing field of photoinduced enantioselective [2+2] cycloadditions. To overcome these challenges, continued development of innovative catalysts and ligands, as well as new reaction modes is of great importance.

Author contributions

Q. C. conceptualized the concept, and J.-X. H. and Q. C. wrote the manuscript.

Conflicts of interest

There are no conflicts to declare.

Data availability

No primary research results, software or code have been included, and no new data were generated or analysed as part of this review.

Acknowledgements

Financial support from the National Natural Science Foundation of China (grant no. 22471043 and 22222104), the Shanghai Pilot Program for Basic Research, and Fudan University is gratefully acknowledged.

Notes and references

1 P. M. Dewick, *Medicinal natural products: a biosynthetic approach*, Wiley, Chichester, UK, 2009.
2 R. D. Taylor, M. MacCoss and A. D. G. Lawson, *J. Med. Chem.*, 2014, **57**, 5845–5859.
3 S. Vaz Jr, *Sustainable agrochemistry: a compendium of technologies*, Springer, Cham, Switzerland, 2019.
4 J. Wu, W. Pisula and K. Müllen, *Chem. Rev.*, 2007, **107**, 718–747.
5 O. Diels and K. Alder, *Justus Liebigs Ann. Chem.*, 1928, **460**, 98–122.
6 G. Brieger and J. N. Bennett, *Chem. Rev.*, 1980, **80**, 63–97.
7 W. Oppolzer, *Angew. Chem., Int. Ed. Engl.*, 1984, **23**, 876–889.

 This journal is © The Royal Society of Chemistry 2026

Open Access Article. Published on 13 2026. Downloaded on 08/05/26 22:54:22.
This article is licensed under a Creative Commons Attribution 3.0 Unported Licence.

8 J. D. Winkler, *Chem. Rev.*, 1996, **96**, 167–176.
9 K. C. Nicolaou, S. A. Snyder, T. M. Montagnon and G. Vassilikogiannakis, *Angew. Chem., Int. Ed.*, 2002, **41**, 1668–1698.
10 K. Takao, R. Munakata and K. Tadano, *Chem. Rev.*, 2005, **105**, 4779–4807.
11 Q. Cai, *Chin. J. Chem.*, 2019, **37**, 946–976.
12 J. Huang, R. Yin and T. Cao, *Acta Chim. Sin.*, 2025, 83, DOI: 10.6023/A25040131.
13 Y. Ma, Y. Wang, F. Wang, S. Lu and X. Chen, *Chin. Chem. Lett.*, 2025, **36**, 110546.
14 R. Hoffmann and R. B. Woodward, *J. Am. Chem. Soc.*, 1965, **87**, 2046–2048.
15 R. B. Woodward and R. Hoffmann, *Angew. Chem., Int. Ed. Engl.*, 1969, **8**, 781–853.
16 R. Hoffmann and R. B. Woodward, *Acc. Chem. Res.*, 1968, **1**, 17–22.
17 K. Fukui, T. Yonezawa and H. Shingu, *J. Chem. Phys.*, 1952, **20**, 722–725.
18 K. Fukui, in A Simple Quantum-Theoretical Interpretation of the Chemical Reactivity of Organic Compounds, *Molecular Orbitals in Chemistry, Physics, and Biology*, Academic Press, New York, 1964, pp. 513–537.
19 K. N. Houk, *Acc. Chem. Res.*, 1975, **8**, 361–369.
20 S. Hashimoto, N. Komeshima and K. Koga, *J. Chem. Soc., Chem. Commun.*, 1979, 437–438.
21 H. Takemura, N. Komeshima, I. Takahashi, S. Hashimoto, N. Ikota, K. Tomioka and K. Koga, *Tetrahedron Lett.*, 1987, **46**, 5687–5690.
22 H. B. Kagan and O. Riant, *Chem. Rev.*, 1992, **92**, 1007–1019.
23 U. Pindur, G. Lutz and C. Otto, *Chem. Rev.*, 1993, **93**, 741–761.
24 E. J. Corey, *Angew. Chem., Int. Ed.*, 2002, **41**, 1650–1667.
25 W. Notz, F. Tanaka and C. F. Barbas, *Acc. Chem. Res.*, 2004, **37**, 580–591.
26 G. Desimoni, G. Faita and K. A. Jørgensen, *Chem. Rev.*, 2006, **106**, 3561–3651.
27 K. Ishihara, M. Fushimi and M. Akakura, *Acc. Chem. Res.*, 2007, **40**, 1049–1055.
28 P. Merino, E. Marqués-López, T. Tejero and R. P. Herrera, *Synthesis*, 2010, 1–26.
29 R. Wang and X. Jiang, *Chem. Rev.*, 2013, **113**, 5515–5546.
30 X.-H. Liu, H. Zheng, Y. Xia, L. Lin and X. Feng, *Acc. Chem. Res.*, 2017, **50**, 2621–2631.
31 B. R. Lichman, S. E. O'Connor and H. Kries, *Chem. – Eur. J.*, 2019, **17**, 6864–6877.
32 V. Laina-Martín, J. A. Fernández-Salas and J. Alemán, *Chem. – Eur. J.*, 2021, **27**, 12509–12520.
33 G. Zhao, S. A. Blaszczy and J. Wang, *Green Synth. Catal.*, 2021, **2**, 198–215.
34 M.-M. Xu and Q. Cai, *Chin. J. Org. Chem.*, 2022, **42**, 698–713.
35 T. Bauer, *Molecules*, 2025, **30**, 1978.
36 L. Dell'Amico, A. Vega-Peñaloza, S. Cuadros and P. Melchiorre, *Angew. Chem., Int. Ed.*, 2016, **55**, 3313–3317.
37 K. N. Flesch, A. Q. Cusumano, P.-J. Chen, C. S. Strong, S. R. Sardini, Y. E. Du, M. D. Bartberger, W. A. Goddard III and B. M. Stoltz, *J. Am. Chem. Soc.*, 2023, **145**, 11301–11310.
38 M. Lautens, W. Klute and W. Tam, Transition Metal-Mediated Cycloaddition Reactions, *Chem. Rev.*, 1996, **96**, 49–92.
39 S. Saito and Y. Yamamoto, *Chem. Rev.*, 2000, **100**, 2901–2915.
40 C. Auvert, L. Fensterbank, P. Garcia, M. Malacria and A. Simonneau, *Chem. Rev.*, 2011, **111**, 1954–1993.
41 P. A. Inglesby and P. A. Evans, *Chem. Soc. Rev.*, 2010, **39**, 1954–1993.
42 L.-N. Wang and Z.-X. Yu, *Chin. J. Org. Chem.*, 2020, **40**, 3536–3558.
43 Y. Zhang, Y. Tang and Y.-Y. Zhou, *Chin. J. Org. Chem.*, 2025, **45**, 1–21.
44 A. Fürstner and P. W. Davies, *Angew. Chem., Int. Ed.*, 2007, **46**, 3410–3449.
45 A. Fürstner, *Acc. Chem. Res.*, 2014, **47**, 925–938.
46 E. Jiménez-Núñez and A. M. Echavarren, *Chem. Rev.*, 2008, **108**, 3326–3350.
47 C. Aubert, L. Fensterbank, P. Garcia, M. Malacria and A. Simonneau, *Chem. Rev.*, 2011, **111**, 1954–1993.
48 A. Marinetti, H. Jullien and A. Voituriez, *Chem. Soc. Rev.*, 2021, **41**, 4884–4908.
49 D. Campeau, D. F. León Rayo, A. Mansour, K. Muratov and F. Gagosz, *Chem. Rev.*, 2021, **121**, 8756–8867.
50 Y. Que, W. Lei, Y. Fang, S. He and Y. Chen, *Green Synth. Catal.*, 2024, **5**, 270–276.
51 Z.-C. Chen, Q. Ouyang, W. Du and Y.-C. Chen, *J. Am. Chem. Soc.*, 2024, **146**, 6422.
52 Y. Inoue, *Chem. Rev.*, 1992, **92**, 741–770.
53 S. Poplata, A. Tröster, Y.-Q. Zou and T. Bach, *Chem. Rev.*, 2016, **116**, 9748–9815.
54 F. Strieth-Kalthoff, M. J. James, M. Teders, L. Pitzer and F. Glorius, *Chem. Soc. Rev.*, 2018, **47**, 7190–7202.
55 J. Großkopf, T. Kratz, T. Rigotti and T. Bach, *Chem. Rev.*, 2022, **122**, 1626–1653.
56 M. Zhu, X. Zhang, C. Zheng and S.-L. You, *Acc. Chem. Res.*, 2022, **55**, 2510–2525.
57 Y. Yin, M. You, X. Li and Z. Jiang, *Chem. Soc. Rev.*, 2025, **54**, 2246–2274.
58 R. S. Jolly, G. Luedtke, D. Sheehan and T. Livinghouse, *J. Am. Chem. Soc.*, 1990, **112**, 4965–4966.
59 L. McKinstry and T. Livinghouse, *Tetrahedron*, 1994, **50**, 6145–6154.
60 S. R. Gilbertson and G. S. Hoge, *Tetrahedron Lett.*, 1998, **39**, 2075–2078.
61 S. R. Gilbertson, G. S. Hoge and D. G. Genov, *J. Org. Chem.*, 1998, **63**, 10077–10080.
62 H. Heath, B. Wolfe, T. Livinghouse and S. K. Bae, *Synthesis*, 2001, 2341–2347.
63 A. Falk, L. Fiebig, J.-M. Neudörfl, A. Adler and H.-G. Schmalz, *Adv. Syn. Catal.*, 2011, **353**, 3357–3362.
64 K. Aikawa, S. Akutagawa and K. Mikami, *J. Am. Chem. Soc.*, 2006, **128**, 12648–12649.
65 S.-J. Paik, U. K. Son and Y. K. Chung, *Org. Lett.*, 1999, **1**, 2045–2047.
66 R. Shintani, Y. Sannohe, T. Tsuji and T. Hayashi, *Angew. Chem., Int. Ed.*, 2007, **46**, 7277–7280.

Open Access Article. Published on 13 2026. Downloaded on 08/05/26 22:54:22.
This article is licensed under a Creative Commons Attribution 3.0 Unported Licence.

67 T. Shibata, D. Fujiwara and K. Endo, *Org. Biomol. Chem.*, 2008, **6**, 464–467.
68 Y. Miyauchi, K. Noguchi and K. Tanaka, *Org. Lett.*, 2012, **14**, 5856–5859.
69 R. L.-Y. Bao, J. Yin, L. Shi and L. Zheng, *Org. Biomol. Chem.*, 2020, **18**, 2956–2961.
70 P. A. Wender, T. E. Jenkins and S. Suzuki, *J. Am. Chem. Soc.*, 1995, **117**, 1843–1844.
71 B. M. Trost, D. R. Fandrick and D. C. Dinh, *J. Am. Chem. Soc.*, 2005, **127**, 14186–14187.
72 Y. Han and S. Ma, *Org. Chem. Front.*, 2018, **5**, 2680–2684.
73 Y. Han, A. Qin and S. Ma, *Chin. J. Chem.*, 2019, **37**, 486–496.
74 J. Li and S. R. Gilbertson, *Org. Lett.*, 2021, **23**, 2911–2914.
75 J. Ye, S. Li, B. Chen, W. Fan, J. Kuang, J. Liu, Y. Liu, B. Miao, B. Wan, Y. Wang, X. Xie, Q. Yu, W. Yuan and S. Ma, *Org. Lett.*, 2012, **14**, 1346–1349.
76 X. Huang, T. Cao, Y. Han, X. Jiang, W. Lin, J. Zhang and S. Ma, *Chem. Commun.*, 2015, **51**, 6956–6959.
77 A. Qin, Q. Zhang, H. Qian, Y. Han and S. Ma, *Chin. J. Chem.*, 2021, **39**, 559–565.
78 Y. Han, A. Qin, Q. Zhang, X. Zhang, H. Qian and S. Ma, *Angew. Chem., Int. Ed.*, 2022, **61**, e202211635.
79 M. Murakami, K. Itami and Y. Ito, *J. Am. Chem. Soc.*, 1997, **119**, 7163–7164.
80 M. Murakami, R. Minamida, K. Itami, M. Sawamura and Y. Ito, *Chem. Commun.*, 2000, 2293–2294.
81 C. Spino, J. Crawford, Y. Cui and M. Gugelchuk, *J. Chem. Soc., Perkin Trans. 2*, 1998, 1499–1506.
82 J.-X. He, Q.-T. Lu, T. Zhang, R.-Y. Gao, Y.-S. Cui, Y. Lan and Q. Cai, *Nat. Catal.*, 2025, **8**, 1348–1360.
83 T. Shibata, K. Takasaku, Y. Takesue, N. Hirata and K. Takagi, *Synlett*, 2002, 1681–1682.
84 B. M. Trost, R. E. Brown and F. D. Toste, *J. Am. Chem. Soc.*, 2000, **122**, 5877–5878.
85 D. Kosser and N. Cramer, *J. Am. Chem. Soc.*, 2015, **137**, 12478–12481.
86 D. Kosser and N. Cramer, *Chima*, 2017, **71**, 186–189.
87 Y. Tamaru, *Modern organonickel chemistry*, Wiley-VCH, Weinheim, German, 2005.
88 P. A. Wender and I. C. Nathan, *J. Am. Chem. Soc.*, 1986, **108**, 4678–4679.
89 P. A. Wender and T. E. Jenkins, *J. Am. Chem. Soc.*, 1989, **111**, 6432–6434.
90 W. Brenner, P. Heimbach, H. Hey, E. W. MüIler and G. Wilke, *Liebigs Ann. Chem.*, 1969, **727**, 161–182.
91 P. Heimbach and H. Schenkhdm, *Top. Curr. Chem.*, 1980, **92**, 45–108.
92 G. Wilke, *Angew. Chem., Int. Ed. Engl.*, 1988, **27**, 185–206.
93 P. J. Garratt and M. Wyat, *J. Chem. Soc., Chem. Commun.*, 1974, 251.
94 I. Suisse, H. Bricout and A. Mortreux, *Tetrahedron Lett.*, 1994, **35**, 413–416.
95 A. EIAmrani, I. Suisse, N. Knouzi and A. Mortreux, *Tetrahedron Lett.*, 1995, **36**, 5011–5014.
96 G. Zhang, C.-Y. Zhao, X.-T. Min, Y. Li, X.-X. Zhang, H. Liu, D.-W. Ji, Y.-C. Hu and Q.-A. Chen, *Nat. Catal.*, 2022, **5**, 708–715.
97 C. Bolm, J. Legros, J. L. Paih and L. Zani, *Chem. Rev.*, 2004, **104**, 6217–6254.
98 A. Correa, O. G. Mancheño and C. Bolm, *Chem. Soc. Rev.*, 2008, **37**, 1108–1117.
99 I. Bauer and H.-J. Knölker, *Chem. Rev.*, 2015, **115**, 3170–3387.
100 P. J. Chirik, *Angew. Chem., Int. Ed.*, 2022, **61**, 5170–5181.
101 E. Braconi, A. C. Götzinger and N. Cramer, *J. Am. Chem. Soc.*, 2020, **142**, 19819–19824.
102 E. Braconi and N. Cramer, *Angew. Chem., Int. Ed.*, 2017, **56**, e202112148.
103 G. Hilt, *Synlett*, 2023, 23–28.
104 P. Röse and G. Hilt, *Synthesis*, 2016, 463–492.
105 W. Hess, J. Treutwein and G. Hilt, *Synthesis*, 2008, 3537–3562.
106 S. Biswas, M. M. Parsutkar, S. M. Jing, V. V. Pagar, J. H. Herbot and T. V. Rajanbabu, *Acc. Chem. Res.*, 2021, **54**, 4545–4564.
107 V. V. Pagar and T. V. Rajanbabu, *Science*, 2018, **361**, 68–72.
108 M. M. Parsutkar, V. V. Pagar and T. V. Rajanbabu, *J. Am. Chem. Soc.*, 2019, **141**, 15367–15377.
109 G. Hilt and F.-X. du Mesnil, *Tetrahedron Lett.*, 2000, **41**, 6757–6761.
110 G. Hilt and K. I. Smolko, *Angew. Chem., Int. Ed.*, 2003, **42**, 2795–2797.
111 G. Hilt, J. Janikowski and W. Hess, *Angew. Chem., Int. Ed.*, 2006, **45**, 5204–5206.
112 D. Singh and T. V. RajanBabu, *Angew. Chem., Int. Ed.*, 2023, **62**, e202216000.
113 K. K. Ghosh, R. Chowdhury, J. P. Gordon and T. V. RajanBabu, *Angew. Chem., Int. Ed.*, 2025, **64**, e202515154.
114 D. J. Gorin, B. D. Sherry and F. D. Toste, *Chem. Rev.*, 2018, **108**, 3351–3378.
115 A. Fürstner, *Chem. Soc. Rev.*, 2009, **38**, 3203–3221.
116 A. S. K. Hashimi, *Angew. Chem., Int. Ed.*, 2010, **49**, 5232–5241.
117 E. Jiménez-Núñez and A. M. Echavarren, *Chem. Commun.*, 2007, 333–346.
118 P. Mauleó, R. M. Zeldin, A. Z. González and F. D. Toste, *J. Am. Chem. Soc.*, 2009, **131**, 6348–6349.
119 I. Alonso, B. Trillo, F. López, S. Montserrat, G. Ujaque, L. Castedo, A. Lledós and J. L. Mascareñas, *J. Am. Chem. Soc.*, 2009, **131**, 13020–13030.
120 A. Z. González and F. D. Toste, *Org. Lett.*, 2010, **12**, 200–203.
121 J. Francos, F. Grande-Carmona, H. Faustino, J. Iglesias-Sigüenza, E. Díez, I. Alonso, R. Fernádez, J. M. Lassaletta, F. López and J. L. Mascareñas, *J. Am. Chem. Soc.*, 2012, **134**, 14322–14325.
122 Y. Wang, P. Zhang, Y. Liu, F. Xia and J. Zhang, *Chem. Sci.*, 2015, **6**, 5564–5570.
123 V. Pirovano, M. Borri, G. Abbiati, S. Rizzato and E. Rossi, *Adv. Synth. Catal.*, 2017, **359**, 1912–1918.
124 M. Nanko, S. Shibuya, Y. Inaba, S. Ono, S. Ito and K. Mikami, *Org. Lett.*, 2018, **20**, 7353–7357.
125 J. M. Keane and W. D. Harman, *Organometallics*, 2005, **24**, 1786–1798.

 This journal is © The Royal Society of Chemistry 2026

Open Access Article. Published on 13 2026. Downloaded on 08/05/26 22:54:22.
This article is licensed under a Creative Commons Attribution 3.0 Unported Licence.

126 B. K. Liebov and W. D. Harman, *Chem. Rev.*, 2017, **117**, 13721–13755.
127 J. A. Smith, K. B. Wilson, R. E. Sonstrom, P. J. Kelleher, K. D. Welch, E. K. Pert, K. S. Westendorff, D. A. Dickie, X. P. Wang, B. H. Pate and W. D. Harman, *Nature*, 2020, **581**, 288–293.
128 K. B. Wilson, J. T. Myers, H. S. Nedzbala, L. A. Combee, M. Sabat and W. D. Harman, *J. Am. Chem. Soc.*, 2017, **139**, 11401–11412.
129 A. W. Lankenau, D. A. Iovan, J. A. Pienkos, R. J. Salomon, S. S. Wang, D. P. Harrison, W. H. Myers and W. D. Harman, *J. Am. Chem. Soc.*, 2015, **137**, 3649–3655.
130 W. Liu, F. You, C. J. Mocella and W. D. Harman, *J. Am. Chem. Soc.*, 2006, **128**, 1426–1427.
131 M. L. Spera, R. M. Chin, M. D. Winemiller, K. W. Lopez, M. Sabat and W. D. Harman, *Organometallics*, 1996, **15**, 5447–5449.
132 B.-X. Xiao, B. Jiang, R.-J. Yan, J.-X. Zhu, K. Xie, X.-Y. Gao, Q. Ouyang, W. Du and Y.-C. Chen, *J. Am. Chem. Soc.*, 2021, **143**, 4809–4816.
133 J.-X. Zhu, Z.-C. Chen, W. Du and Y.-C. Chen, *Angew. Chem., Int. Ed.*, 2022, **61**, e202200880.
134 S.-Z. Tan, P. Chen, L. Zhu, M.-Q. Gan, Q. Ouyang, W. Du and Y.-C. Chen, *J. Am. Chem. Soc.*, 2022, **144**, 22689–22697.
135 P. Chen, S.-Z. Tan, L. Zhu, Q. Ouyang, Z.-J. Jia, W. Du and Y.-C. Chen, *Angew. Chem., Int. Ed.*, 2023, **62**, e202301519.
136 Y.-F. Li, W.-T. Gui, F. Pi, Z. Chen, L. Zhu, Q. Ouyang, W. Du and Y.-C. Chen, *Angew. Chem., Int. Ed.*, 2024, **63**, e202407682.
137 M. A. Ogliaruso, M. G. Romanelli and E. I. Becker, *Chem. Rev.*, 1965, **65**, 261–367.
138 A. Narita, X.-Y. Wang, X. Feng and K. Müllen, *Chem. Soc. Rev.*, 2015, **44**, 6616–6643.
139 X.-Y. Wang, X. Yao and K. Müllen, *Sci. China Chem.*, 2019, **62**, 1099–1144.
140 F. Gavina, A. M. Costero, P. Gil, B. Palazon and S. V. Luis, *J. Am. Chem. Soc.*, 1981, **103**, 1797–1798.
141 P. G. Baraldi, A. Barco, S. Benetti, G. P. Pollini, E. Polo and D. Simoni, *J. Chem. Soc., Chem. Commun.*, 1984, 1049–1050.
142 S. Dong, T. Qin, E. Hamel, J. A. Beutler and J. A. Porco, *J. Am. Chem. Soc.*, 2012, **134**, 19782–19787.
143 X.-X. Yang, R.-J. Yan, G.-Y. Ran, C. Chen, J.-F. Yue, X. Yan, Q. Ouyang, W. Du and Y.-C. Chen, *Angew. Chem., Int. Ed.*, 2021, **60**, 26762–26768.
144 X.-X. Yang, X.-L. Zhao, Q. Ouyang, W. Du and Y.-C. Chen, *Org. Chem. Front.*, 2022, **9**, 1364–1369.
145 J.-L. Cheng, F. Liu, X. Song, Z. Zhao, W. Du and Y.-C. Chen, *J. Org. Chem.*, 2023, **88**, 7800–7809.
146 J.-X. Zhu, F. Pi, T. Sun, W.-Y. Huang, L. Gao, Z.-C. Chen, W. Du and Y.-C. Chen, *Org. Lett.*, 2023, **25**, 3682–3686.
147 Y. Hu, J.-Y. Huang, R.-J. Yan, Z.-C. Chen, Q. Ouyang, W. Du and Y.-C. Chen, *Chem. Sci.*, 2023, **14**, 1896–1901.
148 K. Xie, G.-Q. Zhang, B.-R. Kong, Z.-J. Jia and Z.-C. Chen, *Org. Chem. Front.*, 2024, **11**, 3900–3905.
149 J. Zhang, Y. Hu, T.-Y. Zhang, Z.-C. Chen, W. Du and Y.-C. Chen, *Org. Lett.*, 2023, **25**, 8133–8138.
150 M.-M. Xu and Q. Cai, *Chin. J. Org. Chem.*, 2022, **42**, 698–713.
151 X. Song, Y. Zhang, P. Ji, F. Zeng, F. Bi and W. Wang, *Green Synth. Catal.*, 2020, **1**, 66–69.
152 Y. Zhou, Z. Zhou, W. Du and Y. Chen, *Acta Chim. Sinica*, 2018, **76**, 382–386.
153 M.-M. Xu, P.-P. Xie, J.-X. He, Y.-Z. Zhang, C. Zheng and Q. Cai, *J. Am. Chem. Soc.*, 2024, **146**, 6936–6946.
154 K. Xie, B.-R. Kong, C.-Q. Wang, Z.-C. Chen, W. Du and Y.-C. Chen, *Org. Lett.*, 2025, **27**, 7058–7063.
155 L. F. Tietze, *Chem. Rev.*, 1996, **96**, 115–136.
156 C. K. Prier, D. A. Rankic and D. W. C. MacMillan, *Chem. Rev.*, 2013, **113**, 5322–5363.
157 A. Studer and D. P. Curran, *Angew. Chem., Int. Ed.*, 2016, **55**, 58–102.
158 N. A. Romero and D. A. Nicewicz, *Chem. Rev.*, 2016, **116**, 10075–10166.
159 M. Yan, J. C. Lo and P. S. Baran, *J. Am. Chem. Soc.*, 2016, **138**, 12692–12714.
160 P. Xiong and H. C. Xu, *Acc. Chem. Res.*, 2019, **52**, 3339–3350.
161 J. Huang, R. Ying and T. Cao, *Acta Chim. Sin.*, 2025, **83**, 1424–1434.
162 S. Perveen, L. Qin, M. Zhao, Z. Ding, Y. Wang, Z. Nie and P. Li, *Chin. Chem. Lett.*, 2026, **37**, 111886.
163 D. J. Bellville, D. W. Wirth and N. L. Bauld, *J. Am. Chem. Soc.*, 1981, **103**, 718–720.
164 N. L. Bauld, D. J. Bellville, R. Pabon, R. Chelsky and G. Green, *J. Am. Chem. Soc.*, 1983, **105**, 2378–2382.
165 D. J. Beliviile, N. L. Bauld, R. Pabon and S. A. Gardner, *J. Am. Chem. Soc.*, 1983, **105**, 3584–3588.
166 R. A. Pabon, D. J. Bellville and N. L. Bauld, *J. Am. Chem. Soc.*, 1983, **105**, 5158–5159.
167 G. C. Calhoun and G. B. Schuster, *J. Am. Chem. Soc.*, 1984, **106**, 6870–6871.
168 J. Mlcoch and E. Steckhan, *Angew. Chem., Int. Ed. Engl.*, 1985, **24**, 412–414.
169 A. Gieseler, E. Steckhan, O. Wiest and F. Enoch, *J. Org. Chem.*, 1991, **56**, 1405–1411.
170 T. Horibe, S. Ohama and K. Ishihara, *J. Am. Chem. Soc.*, 2019, **141**, 1877–1881.
171 Y. Yu, Y. Fu and F. Zhong, *Green Chem.*, 2018, **20**, 1743–1747.
172 P. D. Morse, T. M. Nguyen, C. L. Cruz and D. A. Nicewicz, *Tetrahedron*, 2018, **74**, 3266–3272.
173 S. Ohamura, K. Kitagiri, H. Kato, T. Horibe, S. Miyakawa, J. Hasegawa and K. Ishihara, *J. Am. Chem. Soc.*, 2023, **28**, 15054–15060.
174 H. Akao, S. Ohmura and K. Ishihara, *J. Am. Chem. Soc.*, 2026, **148**, 4867–4872.
175 J.-I. Kim and G. B. Schuster, *J. Am. Chem. Soc.*, 1990, **112**, 9635–9637.
176 D. Tian, W. Shi, X. Sun, X. Zhao, Y. Yin and Z. Jiang, *Nat. Commun.*, 2024, **15**, 4563.
177 M. Li, X.-L. Huang, Z.-Y. Zhang, Z. Wang, Z. Wu, H. Yang, W.-J. Shen, Y.-Z. Cheng and S.-L. You, *J. Am. Chem. Soc.*, 2024, **146**, 16982–16989.